WFPC2 Polarization Calibration

J. Biretta and M. McMaster
December 23, 1997

ABSTRACT

We derive a detailed calibration for WFPC2 polarization data which is accurate to about 1.5%. We begin by computing polarizer flats, and show how they are applied to data. A physical model for the polarization effects of the WFPC2 optics is then created using Mueller matrices. This model includes corrections for the instrumental polarization (diattenuation and phase retardance) of the pick-off mirror, as well as the high cross-polarization transmission of the polarizer filter. We compare this model against on-orbit observations of polarization calibrators, and show it predicts relative counts in the different polarizer / aperture settings to 1.5% RMS accuracy. We then show how this model can be used to calibrate GO data, and present two WWW tools which allow observers to easily calibrate their data. Detailed examples are given illustrating the calibration and display of WFPC2 polarization data. In closing we describe future plans and possible improvements.

Table of Contents

1. Introduction

The WFPC2 polarizer filter provides unique wide-field polarimetric imaging capability on HST, and is usable from ~2000Å to ~7000Å. It has been employed on problems ranging from reflection nebulae to the alignment effect in high-z galaxies.

The polarizer filter itself consists of a weak positive lens mounted in a standard square filter wheel slot, with a polarizing coating (POLACOAT) applied to one surface. The filter area is divided into four square "quads," with each having its polarization direction oriented at multiples of 45˚ relative to the other quads (Figure 1). Each of the four quads covers approximately one CCD in the field-of-view, with a ~32 arcsecond wide vignetted region wherever one quad joins another. The polarizer filter can also be rotated slightly by rotating the WFPC2 filter wheel to four positions: -33˚, -18˚, 0˚ (nominal position) and +15˚, though this rotation also has the effect of reducing the usable field-of-view. The non-rotated polarizer filter is selected by specifying filter POLQ in the phase 2 proposal, as well as aperture PC1, WF2, WF3, or WF4, which defines the CCD and filter quad where the target will be placed. Rotated filter positions are similarly selected by specifying filter and aperture combinations as shown in Table 1. Note that polarization angle 0˚ lies roughly along the +X direction (row direction) on PC1 and WF3.

Table 1: Filter Names and Apertures for Polarizer Quad Filter

Filter Name	Aperture Name	FOV Location	Polarization Angle	Comments
POLQ	PC1	PC1	135˚	Nominal filter wheel position
POLQ	WF2	WF2	0˚	Nominal filter wheel position
POLQ	WF3	WF3	45˚	Nominal filter wheel position
POLQ	WF4	WF4	90˚	Nominal filter wheel position
POLQN33	POLQN33	WF2	102˚	Filter wheel rotated -33˚
POLQN18	POLQN18	WF2	117˚	Filter wheel rotated -18˚
POLQP15	POLQP15P	PC1	15˚	Filter wheel rotated +15˚
POLQP15	POLQP15W	WF2	15˚	Filter wheel rotated +15˚

These different apertures and rotations lead to various observing strategies which are fully discussed by Biretta and Sparks (1995). Typically, an observer will take images of the target through three or more different polarizer angles or orientations. These different orientations may be achieved either by selecting different apertures, or by rotating HST to different "ORIENT" angles.

Figure 1: Polarizer Quad Filter. The schematics show the filter projected onto the field-of-view for all rotated positions. Apertures definitions are marked. Dashed lines indicate the central region of each quad which is free of vignetting and cross-talk. Greyscale images are VISFLATs of the polarizer with F555W.

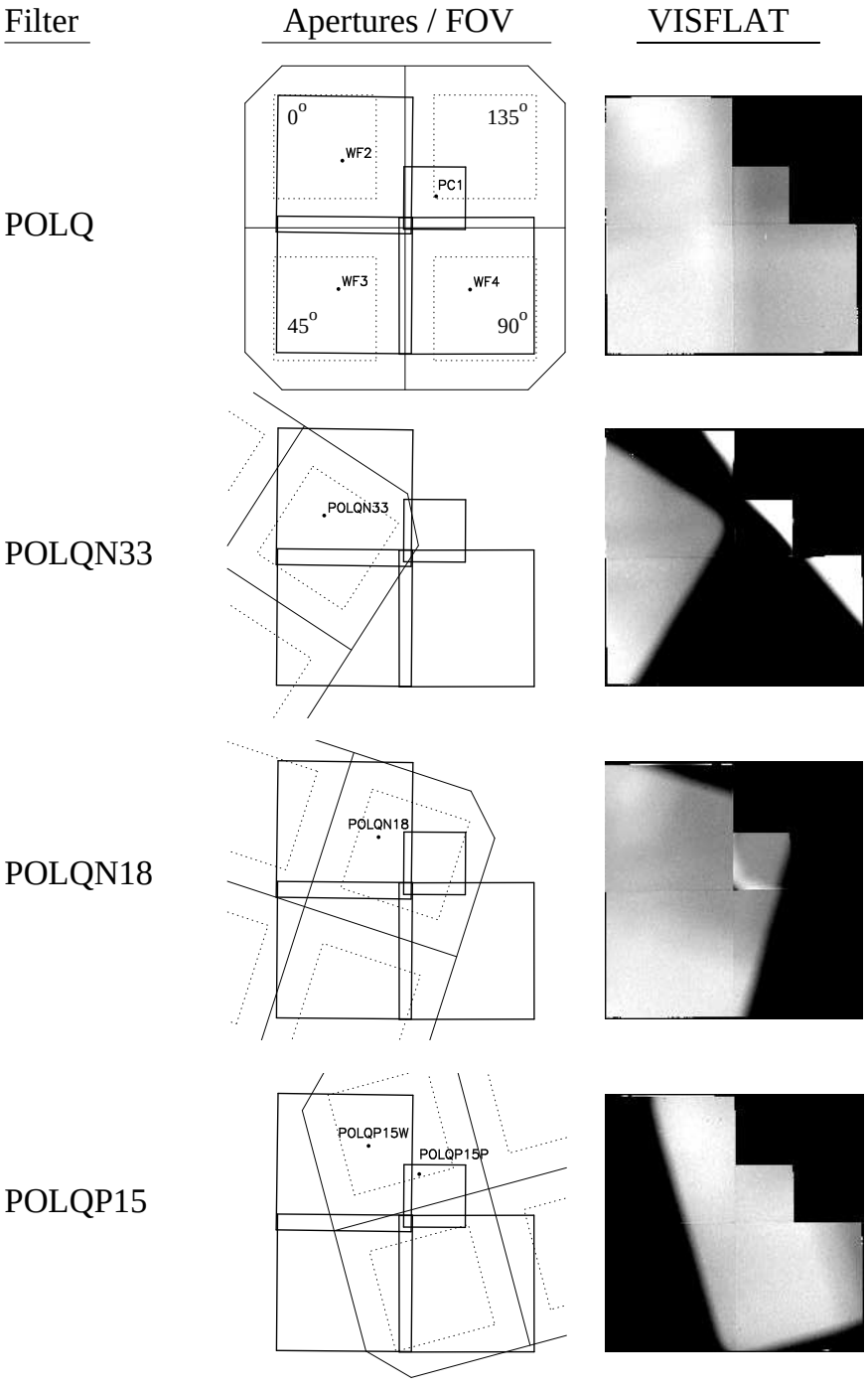

Calibration of WFPC2 polarizer data is a complex problem, and some forethought is needed in developing a calibration strategy. Their are eight possible filter / aperture settings, each of which is characterized by a different polarizer angle. At each of these settings the polarizer has different “parallel” and “perpendicular” transmissions which are functions of wavelength. In addition, the polarizer can be used with any of the 32 spectral filters, each of these has its own transmission curve and usual photometric issues. All these parameters together lead to several hundred possible modes. If we were to calibrate every mode independently, using several targets with different degrees of polarization and using different HST roll angles for each one, it would require over one-thousand HST orbits, which far exceeds that available for WFPC2 calibration. Hence, the central problem is how to calibrate the many possible modes using only the 20 to 30 orbits available for polarization calibration. Our solution will be to develop a detailed physical model for the polarization properties of WFPC2 as a function of wavelength, aperture, polarizer setting, etc. We will then verify this model against a small set of on-orbit data taken in a representative sample of filters and apertures.

Our goal for the accuracy of the WFPC2 polarization calibration is 3% (or 0.03) in the fractional polarization. This was the accuracy stated in early versions of the WFPC2 Handbook, and was the value used in assembling the polarizer science program. Obtaining this level of accuracy will require corrections for two important sources of instrumental polarization in WFPC2: the pick-off mirror and the high perpendicular transmission of the polarizers.

The WFPC2 pick-off mirror consists of an aluminized mirror with an incidence angle of 47˚. Aluminum was chosen since it acts as a good broad-band mirror spanning the UV to near-IR wavebands. However, it is less than ideal for polarization work; it introduces both a spurious polarization, as well as a rotation of the polarization position angle. (Fully-dielectric mirrors are sometimes used in ground-based polarimeters, since they preserve the polarization properties of the incident light.) As we will see, the polarization error can range between 3% to 5% for weakly polarized sources, to as much as 25% for a highly polarized target.

The polarizer filter uses POLACOAT coatings to provide the polarization sensitivity, since these have very good wavefront accuracy, and preserve WFPC2’s near-diffraction-limited imaging. However, these also have high perpendicular transmissions which range from 2% to 15% over the useful wavelength range. (More common materials like those used in sunglasses have perpendicular transmissions of only ~0.3%.) If not properly calibrated, the high perpendicular transmission could lead to large errors in the polarization results.

Hence our detailed strategy can be outlined as follows:

1. Develop a physical model of the WFPC2 optics which allows us to predict the observed counts for any target in any of the available apertures or filters.
2. Include a detailed model of the pick-off mirror and the polarizer, as needed to obtain the required accuracy.
3. Assume all optics other than the pick-off mirror and polarizer filter (i.e. HST mirrors, spectral filters, other WFPC2 optics), have no effect on the polarization properties of the incident light.
4. Assume all WFPC2 and HST optics behave “as designed” with respect to physical properties, transmissions, wavelength dependencies, etc. This eliminates virtually all free parameters in the model, and greatly reduces the amount of on-orbit calibration required.
5. Verify the calibration provided by (1) - (4) against a small number of on-orbit observations in a few spectral filters spanning the useful wavelength range of the polarizers (i.e. F336W, F410M, F555W, and F675W).
6. Perform a more detailed verification at only one wavelength (F555W), where the transmissions of the various quads and apertures are independently tested.

Once such a model is developed and verified, it becomes a simple matter to compute the polarization properties of a given target regardless of the apertures, filters, etc. used.

Observers should recognize that the polarization properties derived for a typical target will be depend on *small* differences (several percent) between images taken in different polarizer settings, different apertures, or different HST roll angles. Any generic WFPC2 problem which affects photometry can potentially have a large impact on polarimetry. The most significant problems of this nature are likely to be the CTE problem, and in the UV, variations in the throughput with time due to contamination. These effects must be corrected either before or during polarization calibration.[1]

In the next section we describe the polarizer flats and their application to data. In Section 3 we derive a model for the polarization properties of WFPC2, and show how it can be used to calibrate observations. In Section 4 we test this model against on-orbit calibrators and show it is accurate to 1.5% RMS. Finally, Sections 5 and 6 present WWW tools for calibration of GO data and give detailed examples.

1. See WFPC2 WWW pages for current discussions of these problems and their correction.

2. Flat Field Calibration

The first step in calibrating polarizer data is to flat field with a reference flat appropriate to the polarizer setting and spectral filter used for the observation. Observers should check that their data were flattened with one of the flats listed below, or otherwise re-calibrate using standard procedures described in the HST Data Handbook.

The polarizer reference flats are available though the HST archive (via STARVIEW, etc.), and the archive file names are given in Table 2. Note that the flats have suffix R4H (i.e. file GA41233FU.R4H) and their data quality files have suffix B4H (i.e. file GA41233FU.B4H). Use the appropriate flat in the table for your spectral filter and polarizer setting. Note that these are multiplicative flats, and are multiplied into the science data during routine calibration.

As with all the WFPC2 flats, the chip-to-chip normalizations are optimized for gain 15. Observations taken at gain 7 will need the usual photometric corrections for differing gain ratios on different CCDs. The corrections are detailed elsewhere (Holtzman, et al. 1995, Whitmore and Heyer 1995, and Biretta 1995).

The regions of the field of view affected by vignetting have been marked in the polarizer flat field data quality files (.B4H files). Observers with extended targets should make sure the target is unvignetted in all their images.

Appendix 1 gives a detailed description of procedures used to generate the polarizer flats.

Table 2: Polarizer Flat Fields

Filter1	Filter2	File
F300W	POLQN18	GA21514JU
F300W	POLQN33	GA21514MU
F300W	POLQP15	GA21514PU
F300W	POLQ	GA21514SU
F336W	POLQN18	GA215151U
F336W	POLQN33	GA215154U
F336W	POLQP15	GA215157U
F336W	POLQ	GA21515BU
F390N	POLQN18	GA21515EU
F390N	POLQN33	GA21515HU
F390N	POLQP15	GA41233FU

Table 2: Polarizer Flat Fields

Filter1	Filter2	File
F390N	POLQ	GA41233IU
F410M	POLQN18	GA41233LU
F410M	POLQN33	GA41233OU
F410M	POLQP15	GA41233QU
F410M	POLQ	GA41233TU
F439W	POLQN18	GA412342U
F439W	POLQN33	GA412345U
F439W	POLQP15	GA412348U
F439W	POLQ	GA41234BU
F547M	POLQN18	GA711082U
F547M	POLQN33	GA711087U
F547M	POLQP15	GA71108BU
F547M	POLQ	GA71108FU
F555W	POLQN18	GA71108KU
F555W	POLQN33	GA71108OU
F555W	POLQP15	GA71108TU
F555W	POLQ	GA711093U
F606W	POLQN18	GA711097U
F606W	POLQN33	GA71109AU
F606W	POLQP15	GA713053U
F606W	POLQ	GA713058U
F656N	POLQN18	GA71305DU
F656N	POLQN33	GA71305HU
F656N	POLQP15	GA71305MU
F656N	POLQ	GA71305RU
F675W	POLQN18	GA713061U
F675W	POLQN33	GA713065U
F675W	POLQP15	GA713069U
F675W	POLQ	GA71306DU

3. Polarimetric Calibration - Theoretical Discussion and Model

In this section we develop a model for the polarization properties of WFPC2 + HST, and describe how it can be used to calibrate data. In the subsequent section we compare the model to on-orbit calibration observations.

There are several notations commonly used to describe the polarization properties of a wavefront, and the polarization action of an optical element. Herein, we will use the Stokes vector and Mueller matrix notations. We find these preferable, since they use only real numbers (i.e. no imaginary numbers), and are thus more easily evaluated by computer.

3.1 The Stokes Vector

The Stokes vector [*I Q U V*] describes the full polarization information of the incident radiation. If E_x and E_y are the real scalar components of the electric field in the *x* and *y* directions, respectively, of a monochromatic wave propagating in the z direction, i.e.:

$$\vec{E} = \left(E_x e^{i\psi_x}\hat{x} + E_y e^{i\psi_y}\hat{y}\right)e^{i(kz-\omega t)}$$

the Stokes vector components may be described as:

$$I = \langle E_x^2\rangle + \langle E_y^2\rangle$$

$$Q = \langle E_x^2\rangle - \langle E_y^2\rangle$$

$$U = \langle 2E_x E_y \cos(\psi_x - \psi_y)\rangle$$

$$V = \langle 2E_x E_y \sin(\psi_x - \psi_y)\rangle$$

where ψ_x and ψ_y are the phases of the corresponding components of the electric field.[2] The first quantity, *I*, is often referred to as the *total intensity*, and is identical to the flux measured during normal (non-polarimetric) photometry. In effect, *Q* compares the strength of the electric vector along the principal axes (*x* and *y*), and is related to the polarization direction. The last two quantities, *U* and *V*, measure the degree of linearity and circularity of the wave, respectively.

2. We note that a wave of finite bandwidth can be decomposed into separate waves, each of which is effectively monochromatic.

The fractional linear polarization of a signal is:

$$p = \frac{\sqrt{(Q^2 + U^2)}}{I}$$

and the position angle of the electric vector of the incident wave (i.e. polarization direction) is given by

$$\chi = \frac{\mathrm{atan}(U/Q)}{2}$$

We note that this choice of definition for χ effectively defines the positive *x*-direction as North, and the positive *y*-direction as East.

We give some illustrative examples of Stokes vectors:

1) An unpolarized wavefront of constant intensity will have some amplitude (say E), but the direction of the E-vector will change randomly over time, and hence we have a Stokes vector (I, Q, U, V) = (E^2, 0, 0, 0).

2) A 100% linearly polarized wave with E-vector at position angle 0, has E_x=E and E_y=0, and hence the Stokes vector is (E^2, E^2, 0, 0).

3) If the wavefront in (2) were instead polarized with the E-vector at position angle 45˚, we have E_x=E_y=E/$\sqrt{2}$. The x and y components of the wavefront are in-phase, and hence (ψ_x - ψ_y) = 0. Hence the Stokes vector is (E^2, 0, E^2, 0).

4) If the wavefront in (2) were instead polarized with the E-vector at position angle 90˚, we have E_x=0 and E_y=E, and the Stokes vector is (E^2, -E^2, 0, 0).

5) If the wavefront is 100% circularly polarized, we have equal intensities in the orthogonal components E_x=E_y=E/$\sqrt{2}$, but they are 90˚ out of phase, so that (ψ_x - ψ_y) = 90˚, and hence we have the Stokes vector (E^2, E^2, 0, E^2).

3.2 Mueller Matrices

Mueller matrices are 4x4 matrices which operate on the Stokes vector, and which can describe the polarization effects of various optical elements, as well as simple coordinate transformations such as rotations. For general discussions of their properties see Kliger, Lewis, and Randall (1990), Chipman (1992a, 1992b), and Collett (1993); a terse discussion of their application to astronomy is given by Seagraves and Elmore (1994).

A simple example of a Mueller matrix operating on a Stokes vector is the following, where [*I Q U V*] describes the wavefront incident on some optical element, and [*I' Q' U' V'*] describes the output wavefront:

$$\begin{bmatrix} I' \\ Q' \\ U' \\ V' \end{bmatrix} = \begin{bmatrix} M_{11} & M_{12} & M_{13} & M_{14} \\ M_{21} & M_{22} & M_{23} & M_{24} \\ M_{31} & M_{32} & M_{33} & M_{34} \\ M_{41} & M_{42} & M_{43} & M_{44} \end{bmatrix} \times \begin{bmatrix} I \\ Q \\ U \\ V \end{bmatrix}$$

One can write a matrix for any single optical element, or multiply together a chain of Mueller matrices to describe the total effect of an optical system. We will utilize them here to describe the WFPC2 pick-off mirror, the polarizer filters, and various rotations between optical elements and/or reference frames.

For our particular application, we can write down a single Mueller matrix which relates the incident Stokes vector to the counts detected by WFPC2. The detected counts for any polarizer observation can be described as the product of the incident Stokes vector and a Mueller matrix *M* representing the total action of all optical components. In general, *M* will be a function of the HST orientation (i.e. PA_V3), the polarizer quad used, and any WFPC2 filter wheel rotation (i.e. θ):

$$C = K \begin{bmatrix} 1 & 0 & 0 & 0 \end{bmatrix} \times M(PA\_V3, \text{quad}, \theta) \times \begin{bmatrix} I \\ Q \\ U \\ V \end{bmatrix}$$

where the scalar constant *K* contains the polarization-independent effects, and the row-vector [1 0 0 0] collapses the Stokes column-vector into the scalar number of detected counts.

The instrumental Mueller matrix can be expanded into separate matrices for various optical elements and rotations between elements. Here we will write Mueller matrices for the WFPC2 polarizers, the WFPC2 pick-off mirror, and rotations of HST and the polarizer fil-

ters. All other optical elements are assumed to have no polarization effects, and are grouped into the scalar constant *K*:

$$C = K\begin{bmatrix}1 & 0 & 0 & 0\end{bmatrix} \times M(pol) \times M(polrot) \times M(POM) \times M(PA\_V3) \times \begin{bmatrix} I \\ Q \\ U \\ V \end{bmatrix}$$

Here *M(pol)* is a Mueller matrix for a generic quad of the polarizer quad filter, *M(polrot*) is a matrix representing rotation of the polarizer quad filter and rotations of individual quads in the filter, *M(POM)* represents the effects of the pick-off mirror, and *M(PA_V3)* represents rotation of the HST spacecraft.

In this situation, *K* includes effects such as the HST aperture size, the HST mirrors, spectral filters, WFPC2 re-imaging optics, CCD quantum efficiency, and WFPC2 amplifier gain. We can recognize that *K* is simply the usual photometric calibration relating incident flux to detected counts for a spectral filter, except for the photometric effects of the pick-off mirror which now are contained in *M(POM)*. Hence the scalar constant *K* can be written as:

$$K = (\text{exposure time}) \times [\text{detected count rate} / \text{incident flux}] / (\text{POM correction})$$

where [detected count rate / incident flux] can readily be computed with SYNPHOT for any spectral filter, and (POM correction) contains the polarization-averaged effects of the WFPC2 pick-off mirror. The scalar term (POM correction) is described further below.

A polarization data set will usually consist of observations in three different combinations of HST orientation, polarizer quad, and filter rotation, thus giving three count rates, and hence three different equations for the three unknowns *I*, *Q*, and *U*. It is then a simple matter to solve for the target properties *I*, *Q*, and *U*. To first order, WFPC2 has no sensitivity to circular polarization; hence *V* cannot be determined, and will be taken to be zero[3]. If observations are made in more than three combinations, the problem becomes over-constrained, and one can fit for *I*, *Q*, and *U*, and an estimate of the statistical errors.

We now derive the individual Mueller matrices in the above equation.

---

3. Ideally, a circularly polarized signal generates equal countrates in all the WFPC2 polarizers, and hence is equivalent to an unpolarized signal. In practice, the phase retardance of the pick-off mirror may convert a circularly polarized signal to an elliptically polarized one, which will have a measurable linearly polarized component. For simplicity we will assume the target has *V*=0.

3.3 The polarizer matrix M(pol)

M(pol) describes the action of the polarizer filter. The general matrix for a non-ideal linear polarizer is given by Seagraves and Elmore (1994)[4]:

$$M(pol) = \begin{bmatrix} [T(par)+T(perp)]/2 & [T(par)-T(perp)]/2 & 0 & 0 \\ [T(par)-T(perp)]/2 & [T(par)+T(perp)]/2 & 0 & 0 \\ 0 & 0 & \sqrt{T(par)T(perp)} & 0 \\ 0 & 0 & 0 & \sqrt{T(par)T(perp)} \end{bmatrix}$$

where *T(par)* and *T(perp*) are the transmissions in the parallel and perpendicular directions, respectively. Elements can be estimated from Figure 2 (c.f. Figure 3.7 in the WFPC2 Instrument Handbook, V. 4, Biretta 1996).

For example, for F555W (effective wavelength 5398Å), *T(par)*=0.6748, *T(perp)*=0.0282, and this is:

$$M(pol) = \begin{bmatrix} 0.3515 & 0.3233 & 0 & 0 \\ 0.3233 & 0.3515 & 0 & 0 \\ 0 & 0 & 0.1381 & 0 \\ 0 & 0 & 0 & 0.1381 \end{bmatrix}$$

4. We note that Morgan, Chipman, and Torr (1990) give a different polarizer matrix with $M_{33} = M_{44} = \sqrt{\frac{T(par)T(perp)}{2}}$, but this appears to be incorrect, since $T(par) = T(perp) = 1$ does not give a unity matrix.

Figure 2: Transmissions *T(par)* and *T(perp*) of the WFPC2 polarizer quad filter as functions of wavelength.

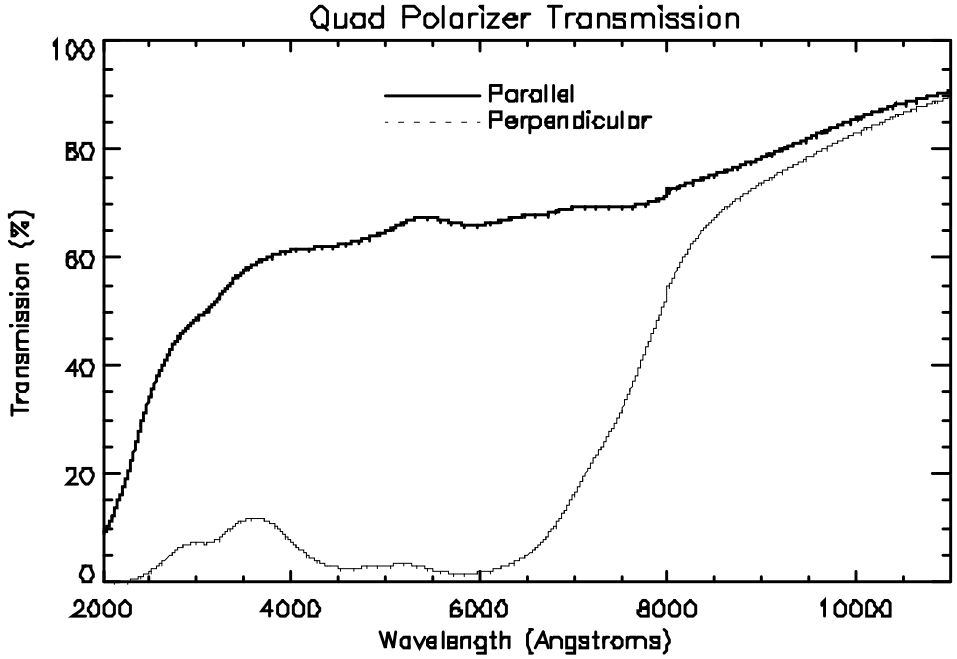

3.4 The polarizer rotation matrix M(polrot)

M(polrot) describes the rotation between the principal axis of the WFPC2 pick-off mirror and the parallel axis of the individual quad of the polarizer filter. This includes rotation of the individual quads within the polarizer filter, as well as the rotation of the entire filter (i.e. filter wheel):

$$M(polrot) = \begin{bmatrix} 1 & 0 & 0 & 0 \\ 0 & \cos(2[\theta - 135]) & \sin(2[\theta - 135]) & 0 \\ 0 & -\sin(2[\theta - 135]) & \cos(2[\theta - 135]) & 0 \\ 0 & 0 & 0 & 1 \end{bmatrix}$$

where θ is given in Table 1 (or Table 3.10 of the WFPC2 Instrument Handbook, Biretta 1996). The angle 135˚ is subtracted, since angles relative to the s-axis of the pick-off mir-

ror are needed (see discussion in next sub-section). For example, for the unrotated POLQ filter on WF3 we have θ=45˚ and the matrix is:

$$M(polrot) = \begin{bmatrix} 1 & 0 & 0 & 0 \\ 0 & -1 & 0 & 0 \\ 0 & 0 & -1 & 0 \\ 0 & 0 & 0 & 1 \end{bmatrix}$$

3.5 The pick-off mirror matrix M(POM)

M(POM) describes the instrumental polarization introduced by the WFPC2 pick-off mirror. The polarization effects of metallic mirrors tend to be rather complicated. In general there are two important effects. First, the reflectance will be different for waves with electric vectors parallel to the mirror surface (transverse electric, TE, or s-wave with reflectance R_s) and normal to this (transverse magnetic, TM, or p-wave with reflectance R_p). This effect is sometimes referred to as "diattenuation." If uncorrected, this can lead to errors as large as 0.04 or 0.05 (4% to 5%) in the fractional polarization derived for a target. Second, reflection at a metal surface will generally convert a linearly polarized wave into an elliptically polarized wave. This process is called "circular retardance," since the phase of the s-wave is retarded relative to the p-wave by an amount we will call $\Delta\phi$ (Chipman 1992). This second effect will be more important for strongly polarized targets, and if uncorrected, can give errors as large as 0.25*p*, where *p* is the fractional polarization of the target.

The Mueller matrix describing these phenomena is (Seagraves and Elmore 1994)[5]:

$$M(POM) = \begin{bmatrix} A & B & 0 & 0 \\ B & A & 0 & 0 \\ 0 & 0 & C & -D \\ 0 & 0 & D & C \end{bmatrix}$$

5. Collett (1992), Ch. 24, eqn. 47 gives the opposite sign on M_{44}, but this seems incorrect since in no case can a unity matrix be obtained.

where

$$A = \frac{(R_s + R_p)}{2}$$

$$B = \frac{(R_s - R_p)}{2}$$

$$C = \sqrt{R_s R_p} \cdot \cos(\Delta\phi)$$

$$D = \sqrt{R_s R_p} \cdot \sin(\Delta\phi)$$

In an effort to illuminate this phenomenon, we consider several simple examples. For a wave at normal incidence $R_s = R_p = R$ and $\Delta\phi = 180°$, so the matrix becomes

$$M = \begin{bmatrix} R & 0 & 0 & 0 \\ 0 & R & 0 & 0 \\ 0 & 0 & -R & 0 \\ 0 & 0 & 0 & -R \end{bmatrix} .$$

Hence the only change in the incident Stokes vector is a reduction of intensity by factor *R*, and a $180°$ phase change in the *U* and *V* components.[6]

For the case of a TE wave at arbitrary incidence angle (i.e. linearly polarized with $\vec{E}$ parallel to the surface), the incident Stokes vector is *(I, I, 0, 0).* Hence, we see that the phase change terms of the Mueller matrix will be unimportant, since *U=V=0.* The outgoing Stokes vector will be *(R_sI, R_sI, 0, 0),* so the only change is a reduction in intensity by R_s.

The case of an incident wave which is purely TM (i.e. linearly polarized with $\vec{B}$ parallel to the surface) is very similar. The incident Stokes vector is *(I, -I, 0, 0),* and so the outgoing Stokes vector is *(R_pI, -R_pI, 0, 0).* Again the only change is a simple intensity reduction.

If we consider the case of a linearly polarized wave which is equally TE and TM, we will see that the situation is much more complex. Such an incident wave has a Stokes vector *(I,0,I,0).* The reflected outgoing wave will then have Stokes vector

---

6. See Kliger, Lewis, and Randall 1990, Section 8.2, for further discussion of this $180°$ phase change. In effect, the $180°$ phase change is equivalent to a mirror reversal of the polarization direction.

$$\left[\quad \left(\frac{R_s + R_p}{2}\right)I \qquad \left(\frac{R_s - R_p}{2}\right)I \qquad (\sqrt{R_s R_p} \cdot \cos\Delta\phi)I \;\; (\sqrt{R_s R_p} \cdot \sin\Delta\phi)I \right] \cdot$$

Hence we see that the properties of the outgoing wave can be completely different from the incident wave. Unless $R_s = R_p$, the emergent wave will have $Q \neq 0$, and hence the plane of polarization will be rotated. Further, depending on the phase change $\Delta\phi$, the emergent wave can be linearly, elliptically, or circularly polarized. For $\Delta\phi$=0 or $180°$ the outgoing wave is linearly polarized (*V=0*), but for $\Delta\phi = 90°$ it is circularly polarized (*U=0)*.[7] The last effect is potentially very important -- any linear polarized intensity which is converted to circular will give the same countrate in all polarizer settings, and hence the fractional polarization derived for the target will be reduced.

We now move on to the calculation of the reflectances R_s and R_p, and the phase retardance $\Delta\phi$, specifically for the WFPC2 pick-off mirror. This mirror consists of evaporated aluminum overcoated with a 250Å thick MgF_2 protective layer.[8] We may compute the R_s, R_p, and $\Delta\phi$ from relations given by Born and Wolfe for a thin dielectric film deposited on a metal surface (Born and Wolfe 1980, Section 13.4.2). The situation is illustrated in the Figure 3 below. The MgF_2 layer is characterized by an index of refraction n_2 and thickness *h*. The aluminum surface is characterized by an index of refraction n_3 and an absorption index κ_3. In Figure 3 $\vec{E}_s$ (coming out of the page) and $\vec{E}_p$ indicate the TE and TM components of the incident electric field, respectively.

Using results given in Born and Wolfe, the ratio of the electric field amplitude for the reflected wave to that of the incident wave is

$$r = \frac{r_{12} + r_{23}e^{i2\beta}}{1 + r_{12}r_{23}e^{i2\beta}}$$

which applies to both the s-wave and p-wave. Since *r* is complex ($i \equiv \sqrt{-1}$), this relationship contains the full phase information. Here r_{12} is the amplitude reflectance at the

---

7. Or approximately circular, if some linear intensity appears in the outgoing Q due to $R_s \neq R_p$.

8. Burrows (1995). Trauger, et al. (1993) describes the coating as a “1300” which is probably a reference to a proprietary Acton Research Corp. #1300 far-UV enhanced Aluminum + MgF_2 coating (Trauger 1997).

Figure 3: Diagram illustrating surface of pick-off mirror. The electric field of the incident s-wave or TE component is denoted by $\vec{E}_s$ (coming out of page), and $\vec{E}_p$ is the p-wave or TM component.

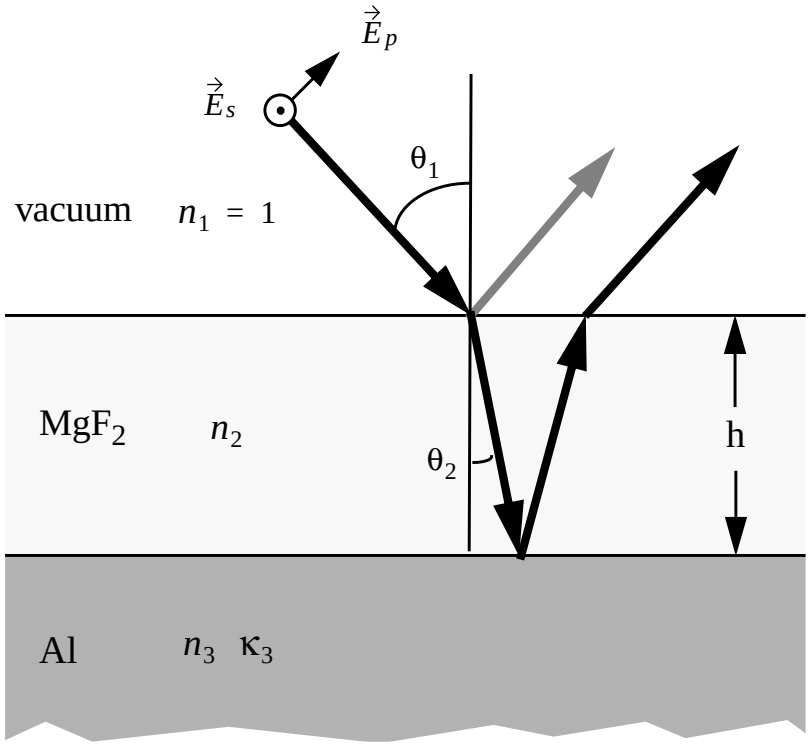

vacuum - dielectric interface, r_{23} is the amplitude reflectance at the dielectric-metal interface, and β is related to the thickness of the dielectric layer. (Herein we will use lower case *r* for the complex reflectance of the electric field *amplitude*, and upper case *R* for the real reflectance of the *intensity.* These are related by $R = r \cdot r^*$.)

We first consider the TE or s-wave. Since there is no absorption in the MgF_2, r_{12} is real and is given by the usual Fresnel equation:

$$(r_{12})_s = \frac{n_1\cos\theta_1 - n_2\cos\theta_2}{n_1\cos\theta_1 + n_2\cos\theta_2}$$

where $n_1 = 1$ for vacuum and n_2 is the index of refraction for the dielectric, in this case MgF_2. The incidence angle of the incoming wavefront is θ_1, where $\theta_1 = 0$ implies normal incidence, and the second angle θ_2 is given by Snell's law, $n_1\sin\theta_1 = n_2\sin\theta_2$.

The metal (aluminum) surface is characterized by both a refractive index n_3 and an absorption index κ_3. In effect, the usual refractive index is replaced by the complex quantity $n_3(1 + i\kappa_3)$. We note that the "extinction coefficient" is sometimes used instead of the absorption index, and is defined as $k_3 = n_3\kappa_3$. The amplitude reflectance of the dielectric - metal interface for the s-wave is given by the complex quantity

$$(r_{23})_s = \frac{n_2\cos\theta_2 - (u + iv)}{n_2\cos\theta_2 + (u + iv)}$$

where

$$2u^2 = Q + \sqrt{(Q^2 + 4n_3{}^4\kappa_3{}^2)}$$

$$2v^2 = -Q + \sqrt{(Q^2 + 4n_3{}^4\kappa_3{}^2)} \text{ and}$$

$$Q = n_3{}^2(1-\kappa_3{}^2) - n_2^2\sin^2\theta_2.$$

For the TM or p-wave the above Fresnel equation becomes

$$(r_{12})_p = \frac{\left(\frac{\cos\theta_1}{n_1}\right) - \left(\frac{\cos\theta_2}{n_2}\right)}{\left(\frac{\cos\theta_1}{n_1}\right) + \left(\frac{\cos\theta_2}{n_2}\right)}$$

and the equation for the MgF_2 - aluminum interface is

$$(r_{23})_p = \frac{[n_3{}^2(1-\kappa_3{}^2) + 2in_3{}^2\kappa_3]\cos\theta_2 - n_2(u + iv)}{[n_3{}^2(1-\kappa_3{}^2) + 2in_3{}^2\kappa_3]\cos\theta_2 + n_2(u + iv)}.$$

Information about the thickness of the dielectric layer is contained in

$$\beta = 2\pi n_2\left(\frac{h}{\lambda_0}\right)\cos\theta_2$$

where λ_0 is the wavelength in vacuum.

Finally the intensity reflectance and phase change for the s-wave are computed as

$$R_s = r_s \cdot r^*_s$$

$$\tan(\phi_s) = \frac{Im(r_s)}{Re(r_s)}$$

and similarly for the p-wave. Here * represents complex conjugation, and *Im* and *Re* represent the imaginary and real parts, respectively. Finally, the retardance of the s-wave relative to the p-wave is

$$\Delta\phi = \phi_s - \phi_p .$$

Given the preceding equations, one can readily calculate the reflectance and phase retardance for any dielectric / metal surface.[9] For our particular case n_2 represents the refractive index of MgF_2. Values are given by Dodge (1984) and are reproduced below in Table 3.

9. See Archer 1962 and Saxena 1965 for helpful examples where SiO_2 is deposited on Si. The inverse problem of deriving physical constants for a material from their polarimetric reflection properties is called Ellipsometry, and references in this area are also useful (e.g. Collett 1993, Ch. 25).

Table 3: Indices of Refraction for MgF_2

Wavelength (Å)	**n**
2000.	1.423
2400.	1.406
2800.	1.396
3200.	1.390
3600.	1.387
4000.	1.384
4400.	1.382
4800.	1.380
5200.	1.379
5600.	1.378
6000.	1.378
6400.	1.3769
6800.	1.3763
7200.	1.3758
7600.	1.3754
8000.	1.3751
8400.	1.3747
8800.	1.3744
9200.	1.3741
9600.	1.3738
10000.	1.3736
14000.	1.3713
18000.	1.3691

The parameters n_3 and k_3 for evaporated aluminum may be found in the AIP Handbook, and are given in Table 4.

Table 4: Indices of Refraction and Extinction Coefficients for Evaporated Aluminum

Wavelength (Å)	**n**	**k**
1200.	0.057	1.15
1400.	0.065	1.43
1600.	0.080	1.73
1800.	0.095	1.97
2000.	0.110	2.20
2200.	0.130	2.40
2400.	0.160	2.53
2600.	0.19	2.85
2800.	0.22	3.13
3000.	0.25	3.33
3200.	0.28	3.56
3400.	0.31	3.80
3600.	0.34	4.01
3800.	0.37	4.25
4000.	0.40	4.45
4360.	0.47	4.84
4500.	0.51	5.00
4920.	0.64	5.50
5460.	0.82	5.99
5780.	0.93	6.33
6500.	1.30	7.11
7000.	1.55	7.00
7500.	1.80	7.12
8000.	1.99	7.05
8500.	2.08	7.15
9000.	1.96	7.70

Setting the incidence angle $\theta_1 = 47^\circ$ and the MgF_2 thickness to h=250Å completes specification of the pick-off mirror. The above equations can be evaluated by a computer program which handles complex numbers, and results in the reflectances and phase retardances shown in the Figure 4 below.

Some discussion about reference frames is needed at this point. Reflection at normal incidence causes a phase retardance of 180˚, which is due effectively to a mirror-reversal of the polarization direction. However, our present analysis of WFPC2 is being done in a reference frame where the mirror-reversal is already removed; in other words, we are working in a co-ordinate system where the field-of-view is projected directly on the sky -- the polarizer axes and rotations, CCD orientations, etc., are all defined in this frame. As a consequence, we need to subtract 180˚ from the phase retardance just derived, before computing the Mueller matrices. In effect, $\Delta\phi$ is replaced by
$\Delta\phi' = 180^\circ - \Delta\phi = 180^\circ - (\phi_s - \phi_p)$.

As an example, we give the Mueller matrix for the pick-off mirror in F555W (effective wavelength 5398Å). From Figure 4 we have R_s=0.9333, R_p=0.8759, and $\Delta\phi$=153.86˚. The Mueller matrix for the pick-off mirror is therefore:

$$M(POM) = \begin{bmatrix} 0.9046 & 0.0287 & 0 & 0 \\ 0.0287 & 0.9046 & 0 & 0 \\ 0 & 0 & 0.8117 & -0.3984 \\ 0 & 0 & 0.3984 & 0.8117 \end{bmatrix}$$

We have also considered whether other mirrors in the optical chain might have important polarization effects, but it appears this is not the case, at least for accuracy levels which are presently relevant. For example, the pyramid mirror has the next largest incidence angle of 9˚, but introduces a spurious polarization of only about R_s - R_p= 0.003 and a phase retardance of about $\Delta\phi'$=1.4˚.

Figure 4: Reflectances R_s and R_p, and phase retardance $\Delta\phi$ computed for pick-off mirror (evaporated aluminum overcoated with 250Å of MgF_2 at 47˚ incidence angle).

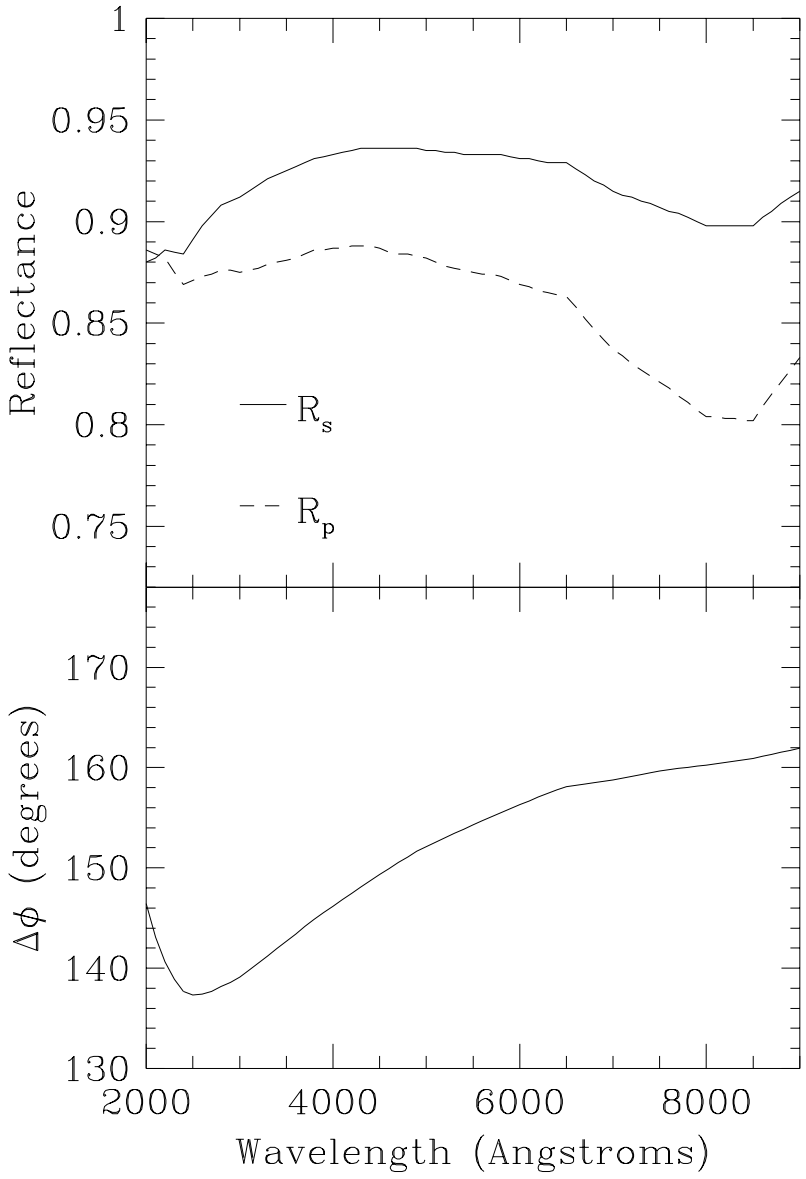

3.6 The HST rotation matrix M(PA_V3)

M(PA_V3) describes the rotation of HST, with the V3 axis used as a reference point:

$$M(\text{PA\_V3}) = \begin{bmatrix} 1 & 0 & 0 & 0 \\ 0 & \cos(2[\text{PA\_V3} + 90]) & \sin(2[\text{PA\_V3} + 90]) & 0 \\ 0 & -\sin(2[\text{PA\_V3} + 90]) & \cos(2[\text{PA\_V3} + 90]) & 0 \\ 0 & 0 & 0 & 1 \end{bmatrix}$$

where PA_V3 is given in the data headers (we add 90˚ since the orientation relative to the s-axis of the pick-off mirror is needed).

For example, for *PA_V3* = 45˚ we have:

$$M(\text{PA\_V3}) = \begin{bmatrix} 1 & 0 & 0 & 0 \\ 0 & -1 & 0 & 0 \\ 0 & 0 & -1 & 0 \\ 0 & 0 & 0 & 1 \end{bmatrix}$$

3.7 Putting it all together

The above matrices can be computed for the circumstances of an observed image, and then multiplied together to produce the single matrix:

$$M(\text{PA\_V3, quad, } \theta) = M(pol) \times M(polrot) \times M(POM) \times M(PA\_V3) =$$

$$\begin{bmatrix} M_{11}(\text{PA\_V3, quad, } \theta) & M_{12}(\text{PA\_V3, quad, } \theta) & M_{13}(\text{PA\_V3, quad, } \theta) & M_{14}(\text{PA\_V3, quad, } \theta) \\ M_{21}(\text{PA\_V3, quad, } \theta) & M_{22}(\text{PA\_V3, quad, } \theta) & M_{23}(\text{PA\_V3, quad, } \theta) & M_{24}(\text{PA\_V3, quad, } \theta) \\ M_{31}(\text{PA\_V3, quad, } \theta) & M_{32}(\text{PA\_V3, quad, } \theta) & M_{33}(\text{PA\_V3, quad, } \theta) & M_{34}(\text{PA\_V3, quad, } \theta) \\ M_{41}(\text{PA\_V3, quad, } \theta) & M_{42}(\text{PA\_V3, quad, } \theta) & M_{43}(\text{PA\_V3, quad, } \theta) & M_{44}(\text{PA\_V3, quad, } \theta) \end{bmatrix}$$

which predicts the observed image as a function of *I*, *Q*, *U*, and *V* images of the target. Note that since the CCD has effectively no polarization sensitivity, only the top row of the product matrix is required. Also, we will assume V=0, since WFPC2 has no sensitivity to circular polarization. Hence the observed target counts are:

$$C = K\{I \cdot M_{11}(\text{PA\_V3, quad, } \theta) + Q \cdot M_{12}(\text{PA\_V3, quad, } \theta) + U \cdot M_{13}(\text{PA\_V3, quad, } \theta)\}$$

Given three observations of a target in different settings of (PA_V3, quad, θ), we have three equations giving three observed counts as a function of Stokes *I, Q,* and *U*. It is then a simple matter to solve this system for the target Stokes parameters. If four or more images are available, a non-linear least squares fit can be done to solve for Stokes *I, Q,* and *U*, along with some empirical estimate of the uncertainties. We note that if one is merely interested in relative quantities, such as the target fractional polarization, *p,* and the polarization position angle, χ, then the photometric calibration constant K becomes unimportant, provided it remains the same between observations.

In this section we have established a model for the WFPC2 polarization properties which allows one to estimate the counts observed for any linearly polarized target. Conversely, the observed counts for a target can be used to solve for its polarization properties. In the next section we examine on-orbit observations of polarizer calibrators, and compare them against this model.

4. Polarimetric Calibration - Comparison of Model to On-Orbit Data

In this section we apply the model of the previous section to on-orbit observations of several polarization calibrators, and compare our results to those in the literature.

Calibration proposal 5574 contains observations of an unpolarized star, G191B2B, a polarized star, BD+64D106, and a polarized reflection nebula, R Mon. Ground-based calibrations for the stars can be found in Schmidt, Elston, and Lupie (1992), and are summarized in Table 5. Ground-based observations of R Mon are presented by Aspin, McLean, and Coyne (1985).

Table 5: Ground-Based Calibrations from Schmidt, Elston, and Lupie (1992)

Target	Filter	p (%)	$\chi(^\circ)$
G191B2B	U	0.065 ± 0.038	92
	B	0.090 ± 0.048	157
	V	0.061 ± 0.038	148
BD+64D106	U	5.110 ± 0.104	97.04 ± 0.58
	B	5.506 ± 0.090	97.15 ± 0.47
	V	5.687 ± 0.037	96.63 ± 0.18
	R	5.150 ± 0.098	96.74 ± 0.54
	I	4.696 ± 0.052	96.89 ± 0.32

The WFPC2 calibration observations were made using the POLQ filter in various settings together with several spectral filters at gain 15. Details are given in Table 6. The images were calibrated in the standard way using the flats listed in Section 2. Cosmic rays were removed by hand, since none of the exposures were CR-SPLIT. For the stars, counts were measured in a 0.5 arcsecond radius aperture. The counts presented in Table 6 have no corrections for CTE effects at this point. Table 7 gives CTE corrections for the polarizer apertures, and are based solely on Y pixel position and an assumed 4% photometric ramp. These corrections are to be multiplied into measured counts.

Table 6: Observations from Calibration Proposal 5574

Image Name	Target	Filter 1	Filter 2	CCD	PA_V3	Exp.T. (s)	Counts
U2M70106T	G191B2B	F336W	POLQ	PC1	286.938	4	3984.
U2M70101T	G191B2B	F336W	POLQ	WF2	286.953	4	3863.
U2M70201T	G191B2B	F336W	POLQ	WF3	289.730	4	3855.
U2M70206T	G191B2B	F336W	POLQ	WF4	289.704	4	3910.
U2M7010BT	G191B2B	F336W	POLQN33	WF2	286.959	4	3734.
U2M7010GT	G191B2B	F336W	POLQP15	WF2	286.947	4	3780.
U2M70107T	G191B2B	F410M	POLQ	PC1	286.938	5	1527.
U2M70102T	G191B2B	F410M	POLQ	WF2	286.953	5	1488.
U2M70202T	G191B2B	F410M	POLQ	WF3	289.730	5	1397.
U2M70207T	G191B2B	F410M	POLQ	WF4	289.704	5	1453.
U2M7010CT	G191B2B	F410M	POLQN33	WF2	286.959	5	1436.
U2M7010HT	G191B2B	F410M	POLQP15	WF2	286.947	5	1463.
U2M70108T	G191B2B	F555W	POLQ	PC1	286.938	1.2	3906.
U2M70103T	G191B2B	F555W	POLQ	WF2	286.953	1.2	3810.
U2M70203T	G191B2B	F555W	POLQ	WF3	289.730	1.2	3721.
U2M70208T	G191B2B	F555W	POLQ	WF4	289.704	1.2	3759.
U2M7010DT	G191B2B	F555W	POLQN33	WF2	286.959	1.2	3742.
U2M7010IT	G191B2B	F555W	POLQP15	WF2	286.947	1.2	3739.
U2M70109T	G191B2B	F675W	POLQ	PC1	286.938	2	3891.
U2M70104T	G191B2B	F675W	POLQ	WF2	286.953	2	3756.
U2M70204T	G191B2B	F675W	POLQ	WF3	289.730	2	3662.
U2M70209T	G191B2B	F675W	POLQ	WF4	289.704	2	3736.
U2M7010ET	G191B2B	F675W	POLQN33	WF2	286.959	2	3738.
U2M7010JT	G191B2B	F675W	POLQP15	WF2	286.947	2	3685.
U2M7030GT	BD+64D106	F336W	POLQ	PC1	225.173	1.4	598.9
U2M70301T	BD+64D106	F336W	POLQ	WF2	225.161	1.4	581.4
U2M70306T	BD+64D106	F336W	POLQ	WF3	225.206	1.4	590.9
U2M7030BT	BD+64D106	F336W	POLQ	WF4	225.206	1.4	611.3
U2M7030LT	BD+64D106	F336W	POLQN33	WF2	225.169	1.4	587.1
U2M7030QT	BD+64D106	F336W	POLQP15	WF2	225.157	1.4	560.9

Table 6: Observations from Calibration Proposal 5574

Image Name	Target	Filter 1	Filter 2	CCD	PA_V3	Exp.T. (s)	Counts
U2M7030HT	BD+64D106	F410M	POLQ	PC1	225.173	1.4	532.1
U2M70302T	BD+64D106	F410M	POLQ	WF2	225.161	1.4	474.5
U2M70307T	BD+64D106	F410M	POLQ	WF3	225.206	1.4	481.3
U2M7030CT	BD+64D106	F410M	POLQ	WF4	225.206	1.4	504.3
U2M7030MT	BD+64D106	F410M	POLQN33	WF2	225.169	1.4	520.5
U2M7030RT	BD+64D106	F410M	POLQP15	WF2	225.157	1.4	472.5
U2M7030IT	BD+64D106	F555W	POLQ	PC1	225.173	0.4	4741.
U2M70303T	BD+64D106	F555W	POLQ	WF2	225.161	0.4	4374.
U2M70308T	BD+64D106	F555W	POLQ	WF3	225.206	0.4	4521.
U2M7030DT	BD+64D106	F555W	POLQ	WF4	225.206	0.4	4783.
U2M7030NT	BD+64D106	F555W	POLQN33	WF2	225.169	0.4	4801.
U2M7030ST	BD+64D106	F555W	POLQP15	WF2	225.157	0.4	4211.
U2M7030JT	BD+64D106	F675W	POLQ	PC1	225.173	0.5	7398.
U2M70304T	BD+64D106	F675W	POLQ	WF2	225.161	0.5	6947.
U2M70309T	BD+64D106	F675W	POLQ	WF3	225.206	0.5	6834.
U2M7030ET	BD+64D106	F675W	POLQ	WF4	225.206	0.5	7286.
U2M7030OT	BD+64D106	F675W	POLQN33	WF2	225.169	0.5	7261.
U2M7030TT	BD+64D106	F675W	POLQP15	WF2	225.157	0.5	6750.
U2M70401T	RMON	F555W	POLQ	PC1, WF2, WF3, WF4	255.250	300	---
U2M70405T	RMON	F555W	POLQ	PC1, WF2, WF3, WF4	255.253	300	---
U2M70409T	RMON	F555W	POLQ	PC1, WF2, WF3, WF4	255.251	300	---
U2M70402T	RMON	F675W	POLQ	PC1, WF2, WF3, WF4	255.250	300	---

Table 6: Observations from Calibration Proposal 5574

Image Name	Target	Filter 1	Filter 2	CCD	PA_V3	Exp.T. (s)	Counts
U2M70403T	RMON	F675W	POLQ	PC1, WF2, WF3, WF4	255.250	300	---
U2M70406T	RMON	F675W	POLQ	PC1, WF2, WF3, WF4	255.253	300	---
U2M7040AT	RMON	F675W	POLQ	PC1, WF2, WF3, WF4	255.251	300	---

Table 7: CTE Corrections for Polarizer Apertures and Stellar Targets

Aperture	CCD	Pixel Y	Multiplicative Correction
POLQ	PC1	424	1.021
POLQ	WF2	414	1.021
POLQ	WF3	424	1.021
POLQ	WF4	421	1.021
POLQN33	WF2	520	1.026
POLQN18	WF2	200	1.010
POLQP15W	WF2	260	1.013

We can then use the equations in Section 3 to predict the counts which should be observed for each calibration data set. These results are given in Table 8. The observed counts are corrected for CTE using Table 7, which is based upon the 4% photometric ramp described by Holtzman, et al. (1995). The uncertainties on the observed counts are estimated at 1% (flat fielding + CTE) plus photon statistical noise added in quadrature. Since we are primarily interested in the polarization properties which are relative quantities, we have normalized the predicted counts so that the mean (pred. - obs.) is zero for each target / spectral filter combination (in effect the photometric constant *K*, or the target brightness, are free parameters).

Table 8: Comparison of Predicted and Observed Counts for Calibrator Stars

Target	Spectral Filter	Pol. Filter	CCD	Predicted Counts (DN)	Observed Counts (DN)	Pred. - Obs. (%)
G191B2B	F336W	POLQ	PC1	3996	4068 ± 42	-1.8 ± 1.1
		POLQ	WF2	3934	3944 ± 42	-0.3 ± 1.1
		POLQ	WF3	3870	3936 ± 42	-1.7 ± 1.1
		POLQ	WF4	3932	3992 ± 42	-1.5 ± 1.1
		POLQN33	WF2	3958	3831 ± 41	3.3 ± 1.1
		POLQP15W	WF2	3902	3829 ± 41	1.9 ± 1.1
BD+64D106	F336W	POLQ	PC1	615	612 ± 9	0.5 ± 1.4
		POLQ	WF2	584	594 ± 9	-1.7 ± 1.4
		POLQ	WF3	585	603 ± 9	-2.9 ± 1.4
		POLQ	WF4	617	624 ± 9	-1.2 ± 1.4
		POLQN33	WF2	621	602 ± 9	3.2 ± 1.4
		POLQP15W	WF2	579	568 ± 8	1.9 ± 1.5
G191B2B	F410M	POLQ	PC1	1520	1559 ± 18	-2.5 ± 1.1
		POLQ	WF2	1490	1520 ± 18	-2.0 ± 1.1
		POLQ	WF3	1459	1427 ± 18	2.3 ± 1.3
		POLQ	WF4	1489	1483 ± 18	0.4 ± 1.2
		POLQN33	WF2	1502	1473 ± 18	2.0 ± 1.2
		POLQP15W	WF2	1475	1482 ± 18	-0.5 ± 1.2
BD+64D106	F410M	POLQ	PC1	522	534 ± 9	-2.2 ± 1.8
		POLQ	WF2	487	484 ± 9	0.7 ± 1.8
		POLQ	WF3	490	491 ± 9	-0.2 ± 1.8
		POLQ	WF4	524	515 ± 9	1.8 ± 1.8
		POLQN33	WF2	529	534 ± 9	-0.9 ± 1.8
		POLQP15W	WF2	482	478 ± 9	0.8 ± 1.8
G191B2B	F555W	POLQ	PC1	3970	3988 ± 42	-0.4 ± 1.1
		POLQ	WF2	3856	3890 ± 42	-0.9 ± 1.1
		POLQ	WF3	3746	3799 ± 41	-1.4 ± 1.1
		POLQ	WF4	3860	3838 ± 41	0.6 ± 1.1
		POLQN33	WF2	3906	3839 ± 41	1.7 ± 1.1
		POLQP15W	WF2	3800	3788 ± 41	0.3 ± 1.1

Table 8: Comparison of Predicted and Observed Counts for Calibrator Stars

Target	Spectral Filter	Pol. Filter	CCD	Predicted Counts (DN)	Observed Counts (DN)	Pred. - Obs. (%)
BD+64D106	F555W	POLQ	PC1	4856	4840 ± 51	0.3 ± 1.1
		POLQ	WF2	4453	4466 ± 47	-0.3 ± 1.1
		POLQ	WF3	4476	4616 ± 49	-3.0 ± 1.1
		POLQ	WF4	4879	4883 ± 50	-0.1 ± 1.1
		POLQN33	WF2	4938	4926 ± 51	0.2 ± 1.1
		POLQP15W	WF2	4386	4266 ± 45	2.8 ± 1.1
G191B2B	F675W	POLQ	PC1	3943	3973 ± 42	-0.8 ± 1.1
		POLQ	WF2	3822	3834 ± 41	-0.3 ± 1.1
		POLQ	WF3	3704	3739 ± 41	-0.9 ± 1.1
		POLQ	WF4	3825	3815 ± 41	0.3 ± 1.1
		POLQN33	WF2	3873	3835 ± 41	1.0 ± 1.1
		POLQP15W	WF2	3762	3733 ± 41	0.8 ± 1.1
BD+64D106	F675W	POLQ	PC1	7518	7553 ± 79	-0.5 ± 1.0
		POLQ	WF2	6962	7092 ± 73	-1.8 ± 1.0
		POLQ	WF3	6934	6978 ± 72	-0.6 ± 1.0
		POLQ	WF4	7490	7439 ± 78	0.7 ± 1.0
		POLQN33	WF2	7586	7450 ± 78	1.8 ± 1.0
		POLQP15W	WF2	6851	6838 ± 71	0.2 ± 1.0

In most cases the model and observed counts agree within 1% to 2% accuracy, though there are a few filter combinations with errors as large as 3%. Table 9 gives the statistics of the agreement. The difference between counts predicted by our polarizer model and the actual calibrator observations is 1.5% RMS across all the data. This is consistent with our goal of 3% accuracy for the polarizer calibration. The RMS values appear to increase as wavelength decreases, and are largest for the F336W filter. This may be due in part to the blue filters having lower sky background and hence larger CTE errors.

The rotated and non-rotated polarizer settings appear to have similar accuracy, although there is a some evidence for the model to predict counts which are too high in the rotated settings (by 1.3% on average).

Table 9: Statistics of (Pred. - Obs.) Counts for Polarizer Model

Filter / Apertures	Mean (Pred. - Obs.)	RMS (Pred. - Obs.)
All	≡0%	1.5%
Un-rotated Pol. Settings	-0.7%	1.3%
Rotated Pol. Settings	1.3%	1.2%
F336W	≡0%	2.0%
F410M	≡0%	1.6%
F555W	≡0%	1.4%
F675W	≡0%	1.0%

If the data were sufficiently robust, one would use these results to derive corrections to the polarizer model. The most obvious correction would be an allowance for the possibility of slightly different transmissions in different quads of the polarizer filter. One will recall that the polarizer flats are normalized with the assumption that all the polarizer apertures have identical transmissions (c.f. Appendix 1). We have attempted to derive such corrections by averaging the (Pred. - Obs.) results in Table 8 for the two calibrator stars, and present the results in Table 10. These corrections would be multiplied into measured counts (or images) before computing the Stokes parameters, and would tend to bring the observations into agreement with the model presented above. The corrections probably do contain some useful information, since the standard deviation of the mean (RMS/2 for the four filters) tends to be less that the magnitude of the corrections. However, they are derived from only one polarized target at a single HST roll angle (as well as a single unpolarized target), and so we feel they are quite preliminary. Additional calibration observations planned for Cycles 6 and 7 should provide a better test of these corrections (see Section 7).

We have also used the data for R MON to derive a polarization map of the surrounding reflection nebula. The resulting image is shown by Figure 5 of the Section 6, and is substantially identical to the ground-based results of Aspin, McLean, and Coyne (1985).

Table 10: Derivation of Preliminary Polarizer Filter / CCD Corrections

Filter	Polarizer Filter / CCD					
	POLQ PC1	**POLQ WF2**	**POLQ WF3**	**POLQ WF4**	**POLQN33 WF2**	**POLQP15W WF2**
F336W	-0.6%	-1.0%	-2.3%	-1.4%	3.2%	1.9%
F410M	-2.4%	-0.6%	1.0%	1.1%	0.5%	0.2%
F555W	0.0%	-0.6%	-2.2%	0.2%	1.0%	1.6%
F675W	-0.6%	-1.1%	-0.8%	0.5%	1.4%	0.5%
Mean (all filters)	-0.9%	-0.8%	-1.1%	0.1%	1.5%	1.0%
RMS (all filters)	1.0%	0.2%	1.5%	1.1%	1.2%	0.8%
Correction	0.991	0.992	0.989	1.001	1.015	1.010

5. Software Tools for Modeling and Calibrating Observations

Currently there are two WWW tools available to aid in polarization calibration. The first tool is essentially a simulator of the WFPC2 polarization properties, and is useful for test purposes and in deriving calibrations. The second tool is designed to calibrate GO data, and gives simple recipes for *I, Q, U,* fractional polarization, and polarization position angle, which can be used to calibrate point sources and images. If aperture counts are given for a target, the second tool will also output the target polarization properties. The inner workings of both tools are described more fully in Appendix 2.

The first tool, or "simulator tool," accepts information for a model target (e.g. total intensity, fractional polarization, and polarization position angle), and circumstances of up to six observed images (PA_V3, polarizer setting, aperture used, spectral filter), and then predicts the observed counts in each image using the above Mueller matrix formalism. The user may optionally provide measured counts and uncertainties for each image, and the program will then estimate the chi-squared between the model and the observed data. In this way, the simulator tool can be used to derive the Stokes parameters for a target, though it will obviously be labor intensive to manually adjust the model and iterate. The simulator tool can be found at:

http://www.stsci.edu/ftp/instrument_news/WFPC2/Wfpc2_pol/wfpc2_pol_sim.html

The second tool, or "calibration tool," accepts the circumstances of three observed images (PA_V3, polarizer setting, aperture used, spectral filter), computes the appropriate Mueller matrices, solves for Stokes *I, Q,* and *U* in terms of the input images, and then outputs simple recipes for *I, Q,* and *U*. The user may optionally input measured aperture counts for some target in each image, and the tool will return values of *I, Q, U,* fractional polarization, and polarization position angle for the target. The calibration tool can be found at:

http://www.stsci.edu/ftp/instrument_news/WFPC2/Wfpc2_pol/wfpc2_pol_calib.html

There is currently no "automatic" facility for estimating the uncertainties due to photon noise. It is suggested that the user try to estimate the noise in their images, add some noise to the image (or to the aperture counts) and repeat the calculations to get an estimate of the effect of photon noise. In general, large coefficients (>few) in the equations for *I, Q,* and *U* will mean high sensitivity to noise, since a small change in one of the observed images makes a large change in the result.

Both tools are accurate to about 1.5% RMS as described in the preceding section, which exceeds our 3% accuracy goal. However, observers should be aware that this accuracy will only be achieved in the absence of other generic WFPC2 problems. The CTE problem may cause lower accuracy in some situations. Specifically, the CTE problem will tend to cause larger errors in images with faint targets or low background counts. The 4% photo-

metric ramp correction we have used for CTE is only a rough approximation (c.f. Whitmore and Heyer 1997). Also, UV observations may require correction for contamination if data are taken at different times, or using different CCDs.

6. Examples for Observers:

Below are two examples showing how to calibrate WFPC2 polarizer data. In the first, the polarization calibration tool is applied to stellar target BD+64D106. The second example shows how to generate Stokes images and polarization vector plots for the reflection nebula surrounding R Mon.

6.1 Stellar Target: BD+64D106

Here observations of the polarization standard star BD+64D106 are considered. The observations were made as part of the calibration proposal 5574. The circumstances of the images are as follows:

Table 11: Circumstances and Measured Counts for BD+64D106

Image Name	Aperture	Polarizer Setting	PA_V3	Observed Counts	CTE Correction	Pol. Filter / CCD Correction	Corrected Counts
u2m70304t	WF2	POLQ	225	7092 ± 73	1.021	0.992	7183 ± 75
u2m70309t	WF3	POLQ	225	6978 ± 72	1.021	0.989	7046 ± 74
u2m7030et	WF4	POLQ	225	7439 ± 78	1.021	1.001	7603 ± 80

The aperture names and polarizer settings come from the phase 2 proposal, the PA_V3 values are from the image headers, and all images used spectral filter F675W.

The images were calibrated with task *calwp2*. The flat field, GA71306DU, was used for all images (F675W + POLQ) and counts were then measured in each image using a 0.5 arcsecond radius aperture. The CTE corrections and polarizer filter corrections from Tables 7 and 10, respectively, were multiplied into the measured counts. The above circumstances and corrected counts were then input into the calibration tool as shown below.[10]

10. We note that SYNPHOT results can be optionally input in the first three blanks of the calibration tool. If these values are left set to zero (the default), the tool will use the polarizer transmission values at the effective wavelength of the spectral filter. This will be quite adequate in most cases. However, in cases where the color of the target is very strong (e.g. M stars) or where the polarizer properties vary strongly across the bandpass of the spectral filter (e.g. F814W), the accuracy can be improved by running the SYNPHOT task *calcphot* to estimate countrates for the spectral filter alone, the spectral filter + POLQ_PAR, and the spectral filter + POLQ_PERP, and then inputting these results here.

WFPC2 POLARIZATION CALIBRATION TOOL:

For help on using this tool, click here. CALCULATE

Give count rate per unit flux from SYNPHOT runs (optional).

Input value or leave set to zero. Click here for help:.

Spectral filter only: 0 . Spectral filter + POLQ_PAR: 0 .

Spectral filter + POLQ_PERP: 0 .

Normally this program will apply a correction to the output which allows using SYNPHOT to convert counts to I, Q, and U calibrated fluxes. Choosing YES will apply this correction; if you do not want it choose NO. Click here for help. YES

Give the spectral filter used: F675W

If using LRF filter, give wavelength also (Ang.):

Give the aperture, POLQ setting, and PA_V3 value for each observed image. If you have measured aperture counts for your target, you can input those, too.

1st image: WF2 POLQ PA_V3 = 225 Counts = 7183

2nd image: WF3 POLQ PA_V3 = 225 Counts = 7046

3rd image: WF4 POLQ PA_V3 = 225 Counts = 7603

RESET FORM | CALCULATE

Please send comments about this form to biretta@stsci.edu.

The user then clicks on the “calculate” button. After about a minute the results below are returned:

WFPC2 Polarization Calibration Tool Results

Final Result

Image	Aperture	Pol. Filter Setting	PA_V3 (deg.)	Counts
1	WF2	POLQ	225.00	7183
2	WF3	POLQ	225.00	7046
3	WF4	POLQ	225.00	7603

SOLVED EQUATIONS:

I = 1.2474 (Image 1) + 0.1331 (Image 2) + 1.2474 (Image 3)

Q = 1.7972 (Image 1) + –0.0000 (Image 2) + –1.7972 (Image 3)

U = –1.6197 (Image 1) + 3.3441 (Image 2) + –1.6197 (Image 3)

DERIVED STOKES PARAMETERS:

I = 19381.8790

Q = –754.8240

U = –386.3556

DERIVED FRACTIONAL POLARIZATION: 4.3750 percent

DERIVED POLARIZATION POSITION ANGLE (E–VECTOR): 103.5528 degrees

This results shows the target is 4.4% polarized at position angle 104˚. By adjusting the input counts up and down to account for their uncertainties, and then re-running the tool several times, we can estimate the error bar on the results. This produces 4.4% ± 0.7% polarization and position angle 104˚± 5˚. This result is in rough agreement with Schmidt,

Elston, and Lupie (1992) who give 5.2% polarization at position angle 97˚ from ground-based data.

6.2 Extended Target: R Mon

Three images of R Mon were taken through the POLQ filter in its unrotated position using CCDs WF2, WF3, and WF4. The uncalibrated .d0h files were retrieved from the HST data archive, and then calibrated using the most recent version of *calwp2*. The F555W+POLQ reference flat GA711093U was used. After calibration, cosmic rays were removed. Since we are dealing with an extended target, we omit the CTE correction.

Data files were as follows:

Table 12: R Mon Data Files

Image	Filters	CCD	PA_V3
u2m70401t	F555W+POLQ	WF2	255.25
u2m70405t	F555W+POLQ	WF3	255.25
u2m70409t	F555W+POLQ	WF4	255.25

Next, it was necessary to remove geometric distortion from the images. This was done using the *wmosaic* task in the *stsdas.hst_calib.wfpc* package in IRAF/STSDAS. Since the three images were also taken at the same *PA_V3*, this has the added effect of rotating the images to the same orientation. There is a small residual distortion remaining from the POLQ filter itself, but this will be ignored.

```
wmosaic  u2m70401t.c0h  u2m70401t.hhh
wmosaic  u2m70405t.c0h  u2m70405t.hhh
wmosaic  u2m70409t.c0h  u2m70409t.hhh
```

At this point the images had the same orientation, but were shifted since they were taken on different CCDs. As shown below the *imcopy* and *imlintran* tasks in the *cl.images* package in IRAF were used to extract aligned 401x401 pixel subimages from the 1600x1600 pixel output image from *wmosaic*. For the *imlintran* task parameters listed below, “xin” and “yin” represent the location of some feature in the input images, and “xout” and “yout” represent the desired position of this feature in the output image.

Extract roughly aligned 401x401 pixel sub-images:

```
imcopy  u2m70401t.hhh[221:621,172:572]  wf2
imcopy  u2m70405t.hhh[964:1364,159:559]  wf3
imcopy  u2m70409t.hhh[959:1359,933:1333]  wf4
```

The task *imlintran* is applied to each image for a more exact alignment.

```
Image Reduction and Analysis Facility

PACKAGE = images

   TASK = imlintran
input   =                  wf3  Input data
output  =                 wf3s Output data
xrotatio=                   0.  X axis rotation in degrees
yrotatio=                   0.  Y axis rotation in degrees
xmag    =                   1.  X output pixels per input pixel
ymag    =                   1.  Y output pixels per input pixel
(xin    =                119.8) X origin of input frame in pixels
(yin    =                105.7) Y origin of input frame in pixels
(xout   =                119.2) X origin of output frame in pixels
(yout   =                104.7) Y origin of output frame in pixels
(ncols  =                 401.) Number of columns in the output image
(nlines =                 401.) Number of lines in the output image
(interpo=               linear) Interpolant (nearest,linear,poly3,poly5,spline3)
(boundar=              nearest) Boundary extension (nearest,constant,reflect,wra
(constan=                   0.) Constant boundary extension
(fluxcon=                  yes) Preserve image flux?
(nxblock=                  256) X dimension of blocking factor
(nyblock=                  256) Y dimension of blocking factor
(mode   =                   ql)
```

Finally, *imlintran* was used again to rotate the aligned images to north-up orientation. This step is crucial to insure the polarization vectors are properly oriented on the image. A careful look at Figure 3.11 in the WFPC2 Handbook (v.4) will convince you that the rotation needed for a *wmosaic* image is approximately PA_V3 - 225˚ = 255.25˚ - 225˚ = 30.25˚ (accuracy about 0.2˚). This was done to all three of the images using inputs shown below. The output images are 500x500 pixels.

```
Image Reduction and Analysis Facility

PACKAGE = images

   TASK = imlintran
input   =                 wf3s  Input data
output  =                 wf3r  Output data
xrotatio=                30.25  X axis rotation in degrees
yrotatio=                30.25  Y axis rotation in degrees
xmag    =                   1.  X output pixels per input pixel
```

```
ymag    =                  1.  Y output pixels per input pixel
(xin    =                200.) X origin of input frame in pixels
(yin    =                200.) Y origin of input frame in pixels
(xout   =                250.) X origin of output frame in pixels
(yout   =                250.) Y origin of output frame in pixels
(ncols  =                500.) Number of columns in the output image
(nlines =                500.) Number of lines in the output image
(interpo=              linear) Interpolant (nearest,linear,poly3,poly5,spline3)
(boundar=               const) Boundary extension (nearest,constant,reflect,wra
(constan=                 0.) Constant boundary extension
(fluxcon=                yes) Preserve image flux?
(nxblock=                256) X dimension of blocking factor
(nyblock=                256) Y dimension of blocking factor
(mode   =                     ql)
```

Then the WFPC2 polarization calibration tool was used to generate recipes for *I*, *Q*, and *U*. The following inputs were used:

WFPC2 POLARIZATION CALIBRATION TOOL:

For help on using this tool, click here. CALCULATE

Give count rate per unit flux from SYNPHOT runs (optional).

Input value or leave set to zero. Click here for help:.

Spectral filter only: 0. Spectral filter + POLQ_PAR: 0.

Spectral filter + POLQ_PERP: 0.

Normally this program will apply a correction to the output which allows using SYNPHOT to convert counts to I, Q, and U calibrated fluxes. Choosing YES will apply this correction; if you do not want it choose NO. Click here for help. YES

Give the spectral filter used: F555W

If using LRF filter, give wavelength also (Ang.):

Give the aperture, POLQ setting, and PA_V3 value for each observed image. If you have measured aperture counts for your target, you can input those, too.

1st image: WF2 POLQ PA_V3 = 255.25 Counts = 0

2nd image: WF3 POLQ PA_V3 = 255.25 Counts = 0

3rd image: WF4 POLQ PA_V3 = 255.25 Counts = 0

RESET FORM CALCULATE

Please send comments about this form to biretta@stsci.edu.

After clicking on the calculate button, these results were obtained:

WFPC2 Polarization Calibration Tool Results

Final Result

Image	Aperture	Pol. Filter Setting	PA_V3 (deg.)	Counts
1	WF2	POLQ	255.25	0
2	WF3	POLQ	255.25	0
3	WF4	POLQ	255.25	0

SOLVED EQUATIONS:

I = 1.3748 (Image 1) + 0.0982 (Image 2) + 1.3748 (Image 3)

Q = 2.1572 (Image 1) + −2.6952 (Image 2) + 0.4594 (Image 3)

U = 0.7602 (Image 1) + 1.5248 (Image 2) + −2.2406 (Image 3)

To compute images of *I*, *Q*, and *U*, the *imcalc* task in the *stsdas.tools.imgtools* package was used along with the above result from the polarization calibration tool:

```
imcalc  wf2r,wf3r,wf4r  i_pol  “1.375*im1 + 0.098*im2 + 1.375*im3”
imcalc  wf2r,wf3r,wf4r  q_pol  “2.157*im1 - 2.695*im2 + 0.459*im3”
imcalc  wf2r,wf3r,wf4r  u_pol  “0.760*im1 + 1.525*im2 - 2.241*im3”
imcalc  i_pol, q_pol, u_pol  f_pol  “sqrt(im2*im2 + im3*im3) / im1”
```

6.3 Display of Polarization Images - IRAF

Display of the polarization image may be achieved in either STSDAS or AIPS. Those familiar with AIPS may find it simpler to use than STSDAS. First we describe the procedure for STSDAS, and then the procedure for AIPS.

The STSDAS script below will take the three images, i_pol, q_pol, and u_pol, and generate a contour plot of i_pol with polarization vectors superposed on it. The procedure starts by smoothing the images with 10x10 pixel block averaging, since we want the plotted vectors (*e.g.*) 10 pixels apart. It then computes images of the fractional polarization and polarization direction, converts these to an STSDAS table and then an ascii text table, and finally plots the ascii table with *fieldplot*. Some care is required to assure the vectors are properly registered on the contour plot (note *tcalc* computation for X and Y pixel numbers), and *vx1*, *vx2*, *vy1*, and *vy2* parameters in *contour* must be carefully chosen to obtain the proper aspect ratio. The output is a postscript file called pol.ps. This script is available at
http://www.stsci.edu/ftp/instrument_news/WFPC2/Wfpc2_pol/wfpc2_pol_display_script

```
#
# stsdas command script to generate contour plot with pol vectors superimposed
#
# average images in 10x10 pixel blocks; plot vectors will be 10 pixels apart
blkavg i_pol i_pol_10 10 10 option="average"
blkavg q_pol q_pol_10 10 10 option="average"
blkavg u_pol u_pol_10 10 10 option="average"
#
# compute fractional pol and direction
stsdas
tools
imgtools
# compute fractional polarization with clipping; set f_pol to zero
# in regions with i_pol_10<5 to keep plot tidy
imcalc i_pol_10,q_pol_10,u_pol_10 f_pol.hhh \
   "if im1.gt.5 then sqrt(im2*im2+im3*im3)/im1 else 0."
# compute polarization direction; correct for degeneracy in atan function,
# and add 90 deg since fieldplot measures angles from plot horizontal axis
imcalc i_pol_10,q_pol_10,u_pol_10 d_pol.hhh \
   "if (im2.ge.0.) then 57.3 * atan(im3/im2) / 2.0 + 90.\
   else 57.3 * atan(im3/im2) / 2.0 + 180."
#
# generate table needed by fieldplot
bye
ttools
# make table with X, Y, fractional pol;
```

```
# wcs=logical means use actual pixel numbers from image
imtab f_pol pol.tab pol_frac pname="x" wcs="logical"
# add pol direction to the table
imtab d_pol pol.tab pol_dir
# correct pixel numbers in table for 10x10 blkavg to assure registration
tcalc "pol.tab" "x" "10*(x1-1)+5" datatype=real
tcalc "pol.tab" "y" "10*(x2-1)+5" datatype=real
# convert iraf table to ascii text table
tdump pol.tab datafile=pol.dat columns="x y pol_frac pol_dir"
#
# generate contour plot
# adjust vx1, vx2, vy1, vy2 to get proper aspect ratio and placement on page
contour i_pol floor=0. ceiling=200. zero=0. ncontou=10 \
    interva=0. nhi=-1 dashpat=528 device=stdgraph \
    title="R Mon" preserv+ label- fill- xres=64 yres=64 perimet+ \
    vx1=0.1 vx2=0.9 vy1=0.2 vy2=0.818 subsamp- append- >>G pol.meta
#
# overlay vector plot onto contours
bye
bye
graphics
stplot
fieldplot pol.dat rtheta+ degrees+ magscal=50 crdpsn="center" \
   head- headsiz=0.0075 psnmark=INDEF marksize=0.0075 zeroplo+ \
   axes- margin- title='R Mon' dvpar.device='imdr' \
   dvpar.append+ dvpar.left=0 dvpar.right=0 \
   dvpar.bottom=0 dvpar.top=0 >>G pol.meta
#
# convert meta-script to postscript
psikern pol.meta devic=psi_port output=pol.ps
```

This procedure will generate the plot shown below in Figure 5. Detailed descriptions of the tasks and their parameters can be found in the IRAF help files (e.g. type *help fieldplot*, etc.).

Figure 5: Polarization display for R Mon. Vectors proportional to fractional polarization (smoothed in 10 x10 pixel boxes) are superposed on contours of total intensity. X and Y coordinates are pixels numbers on the unsmoothed image. North is up; East is left.

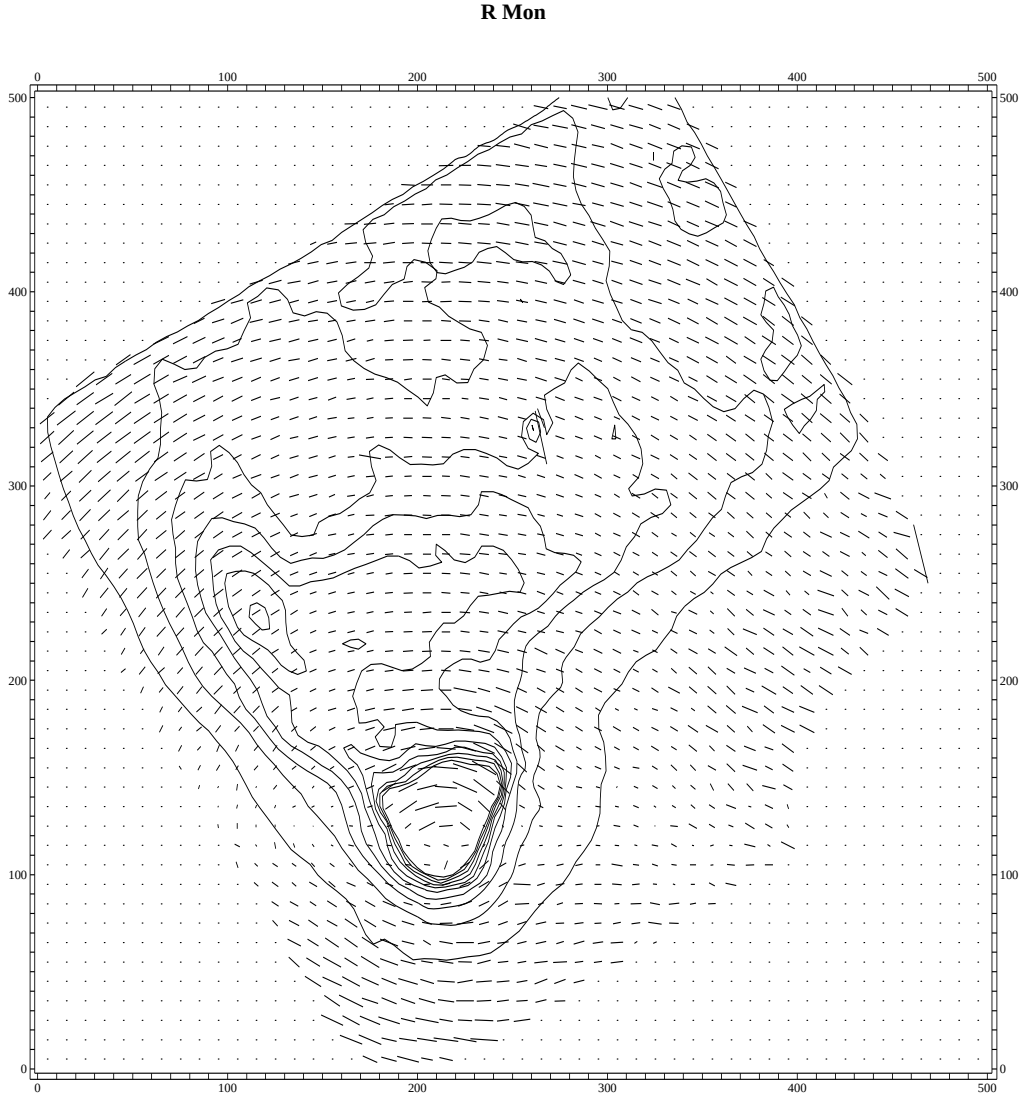

6.4 Display of Polarization Images - AIPS

The AIPS software package from NRAO can also be used for display. Once the images are ported to AIPS in the proper format, the *pcntr* task which is specifically designed for polarization work can be used.

To get the data into AIPS, the I, Q, U, and fractional polarization images need to be converted to FITS format. This can be done using the *wfits* task in *cl.dataio* in IRAF with the following command (note that the output file name must have capital letters). Here is an example for the I image:

```
wfits  i_pol.hhh  IPOL
```

Then start AIPS in another window. When it is up, type “free” which will give a list of disks and available space:

```
>free
AIPS 1: Disk Volume name              Total   Full   Free   Timd Access
AIPS 1:   #                           blocks    %    blocks days
AIPS 1:   1  /ubach/data1/DA01         963342   68   280125  99.0 Alluser
AIPS 1:   2  /ubach/data2/DA01        1759749   57   686336  99.0 Alluser
AIPS 1:   3  /ubach/data3/DA01        3940910   77   808735  99.0 Alluser
```

Disk 3 has the most space. Go back to the IRAF window and type:

```
!cp  IPOL.fits   /ubach/data3/DA01/IPOL.FITS
```

and similar commands for the other Stokes images, which copies the files to where AIPS can get them. Next, read the data into AIPS using *imlod*. Note that DA03 is specified since the data are on the third AIPS disk.

```
>task ‘imlod’
>outnam ‘rmon’
>outcl ‘ipol’
>outdisk 3
>infile ‘da03:ipol.fits’
```

```
>input imlod
AIPS 1: IMLOD:  Task to store an image from a FITS or IBM-CV tape
AIPS 1: Adverbs         Values            Comments
AIPS 1: ------------------------------------------------------------
AIPS 1: INTAPE        1                   Input tape drive # (0 => 1)
AIPS 1: OUTNAME    'RMON        '         Image name (name)
AIPS 1: OUTCLASS   'IPOL  '               Image name (class)
AIPS 1: OUTSEQ        0                   Image name (seq. #)
AIPS 1:                                      0 => highest unique number
AIPS 1:                                     -1 => FITS tape value
AIPS 1: OUTDISK       3                   Disk drive # (0 => any)
AIPS 1: NCOUNT        0                   Number of files to load.
AIPS 1: DOTABLE       1                   True (1.0) means load tables
AIPS 1: NFILES        0                   # of files to advance on tape
AIPS 1: NMAPS         1                   # IBM maps to advance on tape
AIPS 1: INFILE     'DA03:I_POL.FITS       Disk file name (FITS only)
AIPS 1:
AIPS 1:

>go imlod
```

This is repeated for each of the 4 images. AIPS will later become very unhappy if the image scale is not set to the proper value. This is done with the following incantation. Note that the pixel scale on X is negative; this is the AIPS convention for RA. Assuming the first image is in AIPS disk 3, catalog number 1:

```
>indisk 3; getn 1
>keyword='cdelt1'; keyval=-0.09965/3600.,0; puth
>keyword='cdelt2'; keyval= 0.09965/3600.,0; puth
>imhead

AIPS 1: Image=I_POL[1/  (MA)         Filename=RMON        .IMAP  .   1
AIPS 1: Telescope=                   Receiver=WFPC2
AIPS 1: Observer=                    User #= 1103
AIPS 1: Observ. date=05-FEB-1995     Map date=25-JAN-1997
AIPS 1: Minimum= 0.00000000E+00      Maximum= 1.08949385E+04
AIPS 1: ------------------------------------------------------------------
AIPS 1: Type    Pixels   Coord value     at Pixel     Coord incr   Rotat
AIPS 1: RA---TAN   500    06 39 09.980     214.00      -0.099650    0.00
AIPS 1: DEC--TAN   500    08 44 23.700     115.00       0.099650    0.00
AIPS 1: ------------------------------------------------------------------
AIPS 1: Coordinate equinox 1950.00
AIPS 1: Maximum version number of extension files of type HI is   1
```

The last command will display the modified header, so that the correct image scale can be checked. This is repeated for the other 3 polarization images.

An image of the polarization angle direction needs to be computed. For this, use the *comb* task in AIPS. The dialog might look something like below.

```
>task ‘comb’
>indisk 3; mcat
AIPS 1: Catalog on disk 3
AIPS 1:  Cat Usid Mapname Class   Seq  Pt     Last access      Stat
AIPS 1:    1 1103 RMON   .IPOL  .    1 MA 27-JAN-1997 19:00:29
AIPS 1:    2 1103 RMON   .QPOL  .    1 MA 27-JAN-1997 19:23:22
AIPS 1:    3 1103 RMON   .UPOL  .    2 MA 27-JAN-1997 19:23:22
AIPS 1:    4 1103 RMON   .FPOL  .    1 MA 27-JAN-1997 19:23:03
```

[note that the Q image is in catalog slot number 2, and the U image is in number 3:]

```
>indisk 3; getn 2; in2disk 3; get2 3
>outnam ‘rmon’; outcl ‘pola’
>doalign=-2; opcode ‘pola’
>blc 0; trc 0; aparm 0; bparm 0
```

```
>inp
AIPS 1: COMB: Task to combine in many ways two overlapping images
AIPS 1: Adverbs         Values            Comments
AIPS 1: ------------------------------------------------------------------
AIPS 1: USERID        0                   User ID. 0 => current user,
AIPS 1:                                     32000 => any user.
AIPS 1: INNAME     ‘RMON’                 First image name (name)
AIPS 1: INCLASS    ‘QPOL ‘                First image name (class)
AIPS 1: INSEQ         1                   First image name (seq. #)
AIPS 1: INDISK        3                   First image disk drive #
AIPS 1: IN2NAME    ‘RMON ‘                Second image name (name)
AIPS 1: IN2CLASS   ‘UPOL ‘                Second image name (class)
AIPS 1: IN2SEQ        2                   Second image name (seq. #)
AIPS 1: IN2DISK       3                   Second image disk drive #
AIPS 1: DOALIGN      -2                   Should images be coincident?
AIPS 1:                                   (See HELP.)
AIPS 1: OUTNAME    ‘RMON ‘                Output image name (name)
AIPS 1: OUTCLASS   ‘      ‘               Output image name (class)
AIPS 1: OUTSEQ        0                   Output image name (seq. #)
AIPS 1: OUTDISK       3                   Output image disk drive #
AIPS 1: BLC        *all 0                 Bottom left corner
```

```
AIPS 1: TRC        *all 0                Top right corner
AIPS 1: OPCODE     'POLA'                Algorithm type:
AIPS 1:                                  'SUM ','DIV ','SPIX','POLI',
AIPS 1:                                  'POLA','MULT','OPTD','CLIP'
AIPS 1:                                  'REAL','IMAG','MEAN','RM '
AIPS 1:                                  'POLC'
AIPS 1: APARM      *all 0                Parameters for algorithm:
AIPS 1:                                    (1) - (4) scale and offset
AIPS 1:                                    (8) > 0 => blank with 0.0
AIPS 1:                                    (9) Map1 clip level
AIPS 1:                                    (10) Map2 clip level
AIPS 1:                                    see HELP COMB
AIPS 1: BPARM      *all 0                Noise/control parameters:
AIPS 1:                                    (1) Map1 noise level
AIPS 1:                                    (2) Map2 noise level
AIPS 1:                                    (3) > 0 => output noise
AIPS 1:                                    (4) < 0.5 => clip w inputs
AIPS 1:                                        > 1.5 => clip w S/N
AIPS 1:                                        else => clip w noise
AIPS 1:                                    (5) minimum ok S/N or
AIPS 1:                                        maximum ok noise
AIPS 1:                                    (6) max output noise
AIPS 1:                                    see HELP COMB
>
>go comb
```

Next we generate the contour image with polarization vectors superposed using AIPS task *pcntr* (type *help pcntr* to get a help file). The three input images and other parameters are filled in as below.

```
>task pcntr
```

Set names of I, F, and PA images:

```
>indisk 3; getn 1; in2disk 3; get2 4; in3disk 3; get3 6
```

Plot both contours and vectors:

```
>docont 1; dovect 1
```

Set desired image region in pixels:

```
>blc 100, 83; trc 301, 239
```

Select style of plot:

```
>ltype 8
```

Set contour levels; here we use percent:

```
>plev 1; clev 0; levs 0.5, 1, 2, 3, 4, 6, 8, 10, 15, 20, 30, 40, 60, 80
```

Set length and spacing of vectors:

```
>factor 20; xinc 7; yinc 7
```

Set cutoffs where no vectors are plotted:

```
>pcut 0.003; icut 20
```

```
>inp
AIPS 1: PCNTR:  Task to generate plot file for contour plus pol. vectors
AIPS 1: Adverbs         Values            Comments
AIPS 1: ------------------------------------------------------------
AIPS 1: DOCONT        1                   Draw contours? > 0 => yes
AIPS 1: DOVECT        1                   Draw pol. vectors? > 0 => yes
AIPS 1: USERID        0                   Image owner ID number
AIPS 1:                                   Total intensity image:
AIPS 1: INNAME     'RMON '                  Image name (name)
AIPS 1: INCLASS    'IPOL '                  Image name (class)
AIPS 1: INSEQ         1                    Image name (seq. #)
AIPS 1: INDISK        3                    Disk unit #
AIPS 1:                                   Polarization intensity image:
AIPS 1: IN2NAME    'RMON '                  (name) blank => INNAME
AIPS 1: IN2CLASS   'FPOL '                  (class) blank => 'PPOL'
AIPS 1: IN2SEQ        2                    (seq. #) 0 => high
AIPS 1: IN2DISK       3                    Disk drive #, 0 => any
AIPS 1:                                   Polarization angle image:
AIPS 1: IN3NAME    'RMON '                  (name) blank => INNAME
AIPS 1: IN3CLASS   'POLA '                  (class) blank => 'PANG'
AIPS 1: IN3SEQ        5                    (seq. #) 0 => high
AIPS 1: IN3DISK       3                    Disk drive #, 0 => any
AIPS 1: BLC         100          83       Bottom left corner of images
AIPS 1:               1           1          1           1
AIPS 1:               1
AIPS 1: TRC         301         239       Top right corner of images
AIPS 1:               1           1          1           1
AIPS 1:               1
AIPS 1: XYRATIO       0                   X to Y axis plot ratio. 0=>
AIPS 1:                                   header inc or window ratio.
AIPS 1: LTYPE         8                   Type of labeling: 1 border,
AIPS 1:                                   2 no ticks, 3 standard, 4 rel
AIPS 1:                                   to center, 5 rel to subim cen
AIPS 1:                                   6 pixels, 7-10 as 3-6 with
AIPS 1:                                   only tick labels
AIPS 1:                                   <0 -> no date/time
AIPS 1: PLEV          1                   Percent of peak for levs.
```

```
AIPS 1: CLEV          0                    Absolute value for levs
AIPS 1:                                      (used only if PLEV = 0).
AIPS 1:                                      CLEV=PLEV=0 => PLEV=10
AIPS 1: LEVS          0.5          1       Contour levels (up to 30).
AIPS 1:               2            3          4           6
AIPS 1:               8           10         15          20
AIPS 1:              30           40         60          80
AIPS 1:            *rest 0
AIPS 1: FACTOR        20                    Mult. factor for Pol vector
AIPS 1:                                      (see HELP)
AIPS 1: XINC          7                     X-inc. of Pol vectors. 0=>1
AIPS 1: YINC          7                     Y-inc. of Pol vectors. 0=>1
AIPS 1: PCUT          0.003                 Pol. vector cutoff. P units.
AIPS 1: ICUT         20                     Int. vector cutoff. I units.
AIPS 1: DOALIGN      -2                     Maps must align? > 0 => yes
AIPS 1:                                     See HELP DOALIGN!
AIPS 1: DOCIRCLE     -1                     > 0 => extend ticks to form
AIPS 1:                                     coordinate grid
AIPS 1: INVERS        0                     STar file version number.
AIPS 1: STFACTOR      0                     Scale star sizes: 0 => none.
AIPS 1:                                     > 0 crosses with no labels
AIPS 1:                                     < 0 crosses with labels
AIPS 1: CBPLOT       -1                     Position for beam plot:
AIPS 1:                                      -1: don't plot beam
AIPS 1:                                       1: lower left (default)
AIPS 1:                                       2: lower right
AIPS 1:                                       3: upper right
AIPS 1:                                       4: upper left
AIPS 1:                                       6-9 : fill in a little
AIPS 1:                                      11-14: more filled
AIPS 1:                                      16-19: even more
AIPS 1: DOTV         -1                     > 0 Do plot on the TV, else
AIPS 1:                                     make a plot file
AIPS 1: GRCHAN        0                     Graphics channel 0 => 1.
AIPS 1: TVCORN        0            0        TV pixel location of bottom
AIPS 1:                                     left corner of image 0=> self
AIPS 1:                                     scale, non 0 => pixel scale.
```

```
>go pcntr
```

This will generate either a TV display (input DOTV=1 above) or a disk file which can be used to generate a hardcopy (DOTV=-1). To actually get a hardcopy, the AIPS task *lwpla* needs to be run next; this will send the plot to a printer or make a postscript file on disk. Information about the plot contours and vector scales is plotted if LTYPE=3 is set in *pcntr.*

Finally, unix *xv* and *xfig* were used to assemble the two-panel figure with the gray scale image and contour/vector plot shown in Figure 6.

Figure 6: Polarization results for R Mon. (A) is the total intensity image while (B) shows the polarization E vectors (unsmoothed) superposed on contours of total intensity. A vector one arcsecond long corresponds to 25% polarization. North is up; East is left.

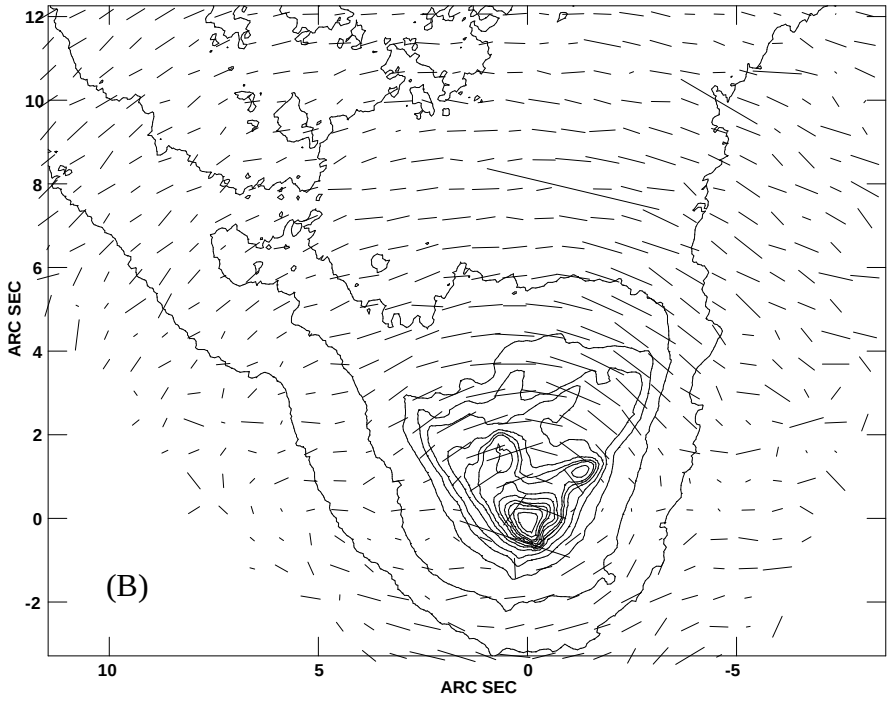

7. Summary and Future Work

In the preceding sections we have developed a model describing the polarization properties of WFPC2 + HST. This model predicts relative counts in different polarizer / aperture settings with 1.5% RMS accuracy, which exceeds our goal of 3% accuracy. We have shown how this model can be used to calibrate GO data, and have presented WWW tools which allow observers to easily calibrate their data.

While the present model and tools should be sufficient for most observers, there remain several areas where further testing and improvements would be useful.

Additional on-orbit observations are needed to verify our model in more spectral filters and apertures, and to allow derivation of more accurate filter / CCD corrections. With additional data, it may be possible to push the calibration accuracy to <1%, so that more difficult observational problems could be addressed. Specifically, proposal 6194 (PI Biretta) will expand upon the calibrations from program 5574 described herein. Observations are made of polarized and unpolarized stars in filter F555W at the PC1, WF2, WF3, and WF4 apertures at four different HST roll angles. These will allow us to measure the properties of each individual quad of the polarizer filter, and test our assumption that the four quads are identical. There are also observations at a single HST roll angle in F300W, F336W, F439W, F675W, and F814W in all the polarizer apertures, to extend the calibration to other wavelengths. Some of these duplicate observations in 5574, while others extend the wavelength coverage farther into the UV or near-IR, or fill-in gaps. Importantly, the new proposal uses CR-SPLITs to avoid potential contamination from cosmic rays; the earlier 5574 observations did not use splitting. There are also VISFLATS to augment the flat fields, and Earth flats are taken in F502N as a check on the overall flat field calibration. These observations should be completed and analyzed by early 1998. A follow-on proposal, 6940, will be executed later if additional tests are needed, and would also test the long-term stability of the calibration.

There are also various practical details we have ignored. The polarizer filter contains a weak lens which will introduce different distortions in the various apertures. Observers with large targets (>20 arcseconds) may need to correct this effect, and so it warrants further study. The polarizer filter may also cause spurious reflections against the spectral filters. While this is unlikely to directly affect GO data, it may have a 1% to 2% effect on the flats. Our scheme for normalizing the flats will remove most of such effects, but again observers with large targets may see some impact far from the aperture centers.

Improvements are also needed in our understanding of the WFPC2 CTE (charge transfer efficiency) problem. This problem affects all WFPC2 data to some extent, but polarization observations are likely to be especially susceptible, since they rely on measuring small dif-

ferences between observations made at different locations on the CCDs. CTE may in fact be the largest error source remaining in the polarization calibration.

With regards future software development, the existing tools need to be tested under more situations, and for more targets. It would also be desirable to add a non-linear least squares solution to the tools, so that 4 or more input aperture counts could be handled. Eventually, it would be desirable to have an advanced STSDAS polarization tool which can automatically align the images and correct geometric distortions (including that caused by the weak lens in the POLQ filter), and then automatically compute *I*, *Q*, and *U* images (and possibly uncertainty images) based solely on information in the image headers.

The Advanced Camera for Surveys (ACS) will be installed in HST in 1999, and will provide a polarization imaging capability similar to that of WFPC2. The algorithms derived above for WFPC2 should also prove useful for ACS. It is likely it will face similar challenges to those in WFPC2, since the current design includes metallic mirrors at near 45˚ incidence angles. Hence ACS should provide additional motivation for theoretical modeling work, and development of advanced polarization tools in STSDAS.

8. References

Archer, R. J., 1962, J. Opt. Soc. Am. 52, 970.

Aspin, C., McLean, I.S., and Coyne, G.V. 1985, Astron. & Astrop. 149, 158.

Beckers, J. M., 1990, *Polarization Considerations for Optical Systems II*, SPIE conference 1166, ed. Chipman, p. 380.

Bevington, P. R. 1969, *Statistical Analysis for the Physical Sciences*.

Biretta, J. A. and Sparks, W. B. 1995, "WFPC2 Polarization Observations: Strategies, Apertures, and Calibration Plans," WFPC2 Instrument Science Report 95-01.

Biretta, J. A. et al. 1996, *WFPC2 Instrument Handbook*, V. 4.0.

Born, M. and Wolf, E., 1985, *Principles of Optics*, (Pergammon Press), Ch. 13.

Burrows, C. 1995, private communication.

Chipman, R. A. 1992a, in *Polarization Analysis and Measurement*, SPIE Proceedings Vol. 1746, p. 49.

Chipman, R. A. 1992b, in *Polarization Analysis and Measurement*, SPIE Proceedings Vol. 1746, p. 62.

Clarke, D. 1974, *Planets, Stars, and Nebulae Studied with Photopolarimetry*, ed. T. Gehrels, (Univ. Arizona press) p. 45.

Collett, E. 1993, *Polarized Light*, (Marcel Dekker, Inc.: New York), Ch. 5.

Dodge, M. J., 1984, Applied Optics 23, 1980.

Engel, J. R., 1992, *Polarization Analysis and Measurement*, SPIE Proceedings Vol. 1746, p. 317.

Holtzman, J. A. et al. 1995, P.A.S.P. 107, 156.

Kliger, D. S., Lewis, J. W., and Randall, C. E., *Polarized Light in Optics and Spectroscopy*, (Academic Press) 1990. Ch. 4 and 5.

Maymon, P. W. and Chipman, R. A., 1992, *Polarization Analysis and Measurement*, SPIE Proceedings Vol. 1746, p. 148.

Morgan, Chipman, and Torr, 1990, *Polarization Considerations for Optical Systems II*, SPIE conference 1166, ed. Chipman, p. 401

Saxena, A. N. 1965, J. Opt. Soc. Am. 55, 1061.

Trauger, J., et al. 1993, “Wide-Field Planetary Camera 2 Instrument Description and User Handbook”, 751-34, Rev. A, JPL D-11212.

Trauger, J. 1997, private communication.

Schmidt, G.D., Elston, R., and Lupie, O.L. 1992, Astron.J. 104, 1563.

Seagraves, P. H. and Elmore, D. F. 1994, *Polarization Analysis and Measurement II*, SPIE Proceedings Vol. 2265, p. 231.

Whitmore, B., and Heyer, I. 1997, “New Results on Charge Transfer Efficiency and Constraints on Flat-Field Accuracy,” WFPC2 Instrument Science Report 97-08.

Appendix 1 - Generation of Polarizer Flat Field Reference Files

The polarizer flats were generated by applying a polarizer correction image to the non-polarizer flat (or “standard flat”) for each spectral filter. The procedure for generation of the “standard flat” is described in the history text accompanying each one. The correction image was derived from the ratio of on-orbit internal VISFLATs taken with and without the polarizer:

$$correction(filter, polfilter) = \frac{VISFLAT(filter + polfilter)}{VISFLAT(filter)}$$

where *filter* = F336W, F410M, or F555W, which are the filters used for the VISFLATs, and *polfilter* = POLQ, POLQN33, POLQN18, or POLQP15.

The VISFLAT(*filter*+*polfilter*) images are from proposal 5574. The VISFLAT(*filter*) images are from proposals 5655 and 5764, and were chosen to be observed within a few days of the polarizer images, so as to minimize time-dependent contamination variations. The raw VISFLAT images were combined in groups of three or four to remove cosmic rays, and then the above ratio was computed.

The correction images were then clipped and median filtered using a 5x5 pixel box to remove individual discrepant pixels which were caused by hot pixels or residual cosmic rays. They were also smoothed with a sigma=5 pixel Gaussian function to further reduce the noise, since there appeared to be no significant features on small scales. Since the polarizers are very far from the focal plane, we do not expect them to contribute any small scale spatial features.

The correction image was then normalized separately for each CCD, so that mean value in the 101x101 pixel region surrounding each of the standard polarizer aperture locations was unity. The aperture positions assumed are listed in Table A1 below. This normalization will remove any spurious throughput differences between apertures which are caused by polarization of the VISFLAT light. (The VISFLAT optics contain several mirrors at incidence angles of 45˚ or shallower.) Any real differences in chip-to-chip polarizer filter throughput will need to be corrected during photometric calibration. To the extent that the four quads of the polarizer are supposedly identical, any such corrections should be very small.

Table A1. Aperture Positions Used to Normalize Polarizer Flats.

Pol. Filter	Aperture	CCD	Pixel
POLQ	PC1 + POS TARG 8,8	PC1	596,596
POLQ	WF2	WF2	424,414
POLQ	WF3	WF3	436,424
POLQ	WF4	WF4	423,421
POLQN33	POLQN33	WF2	292,520
POLQN18	PC1	PC1	410,424
POLQN18	POLQN18	WF2	380,200
POLQP15	POLQP15P	PC1	200,680
POLQP15	POLQP15W	WF2	500,260

Finally the pol. correction images were divided into the standard flats (without polarizers) as follows:

$$polflat(filter, polfilter) = \frac{standardflat(filter)}{polcorrection(filter, polfilter)}$$

We use division here, since the "standard flats" are usually multiplied into the raw data.

Since polarizer VISFLATS were available for only the three filters F336W, F410M, and F555W, we used whichever correction image was closest in wavelength to the "standard flat" filter. Comparison of the different correction images shows that wavelength dependencies are weak, and are likely to contribute errors of about 0.5% RMS when a correction image at one wavelength is applied to a “standard flat” at another wavelength. These errors are largely due to interference fringe patterns with spatial scales >50 pixels. Polarization correction images were applied as in Table A2.

Table A2. Polarization Correction Images Used to Generate the Polarizer Flats.

Pol. Correction (VISFLAT) Filter	Used For Spectral Filter
F336W	F300W
F336W	F336W
F410M	F390N
F410M	F410M
F410M	F439W
F555W	F547M
F555W	F555W
F555W	F606W
F555W	F656N
F555W	F675W

The RMS noise in the polarizer flats is about 0.3% on pixel-to-pixel scales, and is due to the thermal vacuum flat used in generating the “standard flats.”

Photometric Normalizations:

As described above, the polarizer correction images are normalized to unity at the position of each of the standard polarizer apertures. Hence the normalization of the "standard flat" is preserved. The standard flats are taken at gain 15, hence the usual photometric corrections will need to be applied to data taken at gain 7. See Holtzman, et al. 1995, Whitmore and Heyer 1995, and Biretta 1996 for further discussion of the gain corrections during photometry.

The Polarizer Data Quality File:

The polarizer data quality file has marked as "bad" all regions where cross-talk between different segments of the polarizer quad filter will compromise the calibration. Bad pixels and regions from the "standard flat" are also marked.

Future Work:

There is obviously some advantage to using polarization correction images derived in the same filter used for the science observations. Some effort will be made to obtain flatfield

correction images in more filters in Cycles 6 and 7. However, the VISFLAT lamp is slowly burning-out and degrades with each usage, so these flats will need to be prioritized against other calibrations. Earthflats are too bright, except for narrow band filters, and are likely to suffer from strong source polarization.

Appendix 2 - Polarization WWW Software Tools

Herein we briefly summarize the inner workings of the two polarization WWW tools. Both tools are written in the “tcl” language and comprise about 5000 code lines excluding various data tables. The “simulator tool” and “calibrator tool” are separate programs, but have many similarities.

Simulator Tool

The simulator tool is primarily intended for testing the polarizer model and deriving various calibration parameters. For example, it was used to derive “predicted” numbers in Table 8.

The simulator tool consists of the following program units:

- wfpc2-pol-sim.tcl - main program; communications with WWW
- wfpc2-pol-routines.tcl - mueller matrix calculations; polarization routines
- wfpc2-pol-report.tcl - routine to generate output html form
- wfpc2-pol-pom.dat - data table for pick-off mirror reflectance and retardance
- FILTERS/dqe_system.dat - table with WFPC2 CCD DQE curve
- FILTERS/polq_par_sys.dat - table with polarizer parallel throughput curve
- FILTERS/polq_perp_sys.dat - table with polarizer perpendicular throughput curve
- wfpc2.dat - table which serves as index of other WFPC2 data tables
- wfpc2-table-6.2.dat - table containing efficiency and mean wavelength for WFPC2 filter

The user gives the following inputs:

a) The target parameters are input as either (I, p, χ) or (I, Q, U, V). Units are arbitrary, though they should be consistent with any SYNPHOT results provided by the user in (b).

b) Photometric calibration info from SYNPHOT can be optionally input. Specifically three parameters can be input: count rate per flux unit from CALCPHOT for the spectral filter + WFPC2 + HST; count rate per flux unit for the polarizer filter in parallel direction + spectral filter + WFPC2 + HST; and finally count rate per flux unit for the polarizer filter in perpendicular direction + spectral filter

+ WFPC2 + HST. If the user does not specify these, they will be estimated from look-up tables.

c) WFPC2 spectral filter, and wavelength setting if the LRF filter is used.

d) Up to 6 sets of [polarizer / aperture, PA_V3, observed counts, and count uncertainties] may be input. The polarizer / apertures are selected by choosing from a menu.

The following steps are performed during calculation:

1) If (I, p, χ) are given, these are converted to Stokes vector (I, Q, U, V)

2) For the first (polarizer / aperture, PA_V3) setting, compute the Mueller matrix for HST rotation using supplied PA_V3. Apply to Stokes vector.

3) Get filter mean wavelength from look-up table (or just use LRF wavelength). Look up reflectances and phase retardance for pick-off mirror at that wavelength. Compute attenuation matrix for pick-off mirror from physical constants. Apply to current Stokes vector.

4) Compute the angle between the pick-off mirror axis and the polarizer filter axis using (aperture / filter) chosen by user. Compute Mueller matrix for rotation and apply to current Stokes vector.

5) Look up polarizer transmissions for mean wavelength of the spectral filter. If user has input SYNPHOT results for the polarizer, use those instead. Compute Mueller matrix for polarizer. Apply to current Stokes vector.

6) Extract Stokes I from current Stokes vector, which is what CCD detects. If user gave SYNPHOT results, apply the spectral filter result to I, and divide by the mean pick-off mirror transmission.

7) If more than one (polarizer / aperture) setting was supplied, go to (2) and compute for next setting.

8) After all settings are computed, output resulting model counts and any “observed” counts provided by user. Also compute (model - observed) and chi-square.

Calibration Tool

The calibration tool is designed to give observers an easy method for obtaining the polarization properties of their target. Given the circumstances of the observer's images (i.e. polarizer filter and PA_V3), the tool returns a simple recipe for the polarization properties, with full corrections for instrumental errors. If observers also give aperture counts for their target, the tool will directly return the polarization properties.

The calibrator tool consists of the following program units:

- wfpc2-pol-calib.tcl - main program; communications with WWW
- wfpc2-pol-routines.tcl - performs actual calculations
- wfpc2-pol2-report.tcl - routine to generate output html form
- matrix_3.tcl - generic 3x3 matrix arithmetic routines
- matrix_4.tcl - generic 4x4 matrix arithmetic routines
- matinv.tcl - generic 3x3 matrix inversion routine
- utilities.tcl - generic tcl utility routines
- astro.tcl - generic astronomy routines
- wfpc2-pol-pom.dat - data table for pick-off mirror reflectance and retardance
- FILTERS/dqe_system.dat - table with WFPC2 CCD DQE curve
- FILTERS/polq_par_sys.dat - table with polarizer parallel throughput curve
- FILTERS/polq_perp_sys.dat - table with polarizer perpendicular throughput curve
- wfpc2.dat - table which serves as index of other WFPC2 data tables
- wfpc2-table-6.2.dat - table containing efficiency and mean wavelength for WFPC2 filter

The user gives the following inputs, which are a subset of the simulator tool inputs:

a) Photometric calibration info from SYNPHOT can be optionally input. Specifically three parameters can be input: count rate per flux unit from CALCPHOT for the spectral filter + WFPC2 + HST; count rate per flux unit for the polarizer filter in parallel direction + spectral filter + WFPC2 + HST; and finally count rate per flux unit for the polarizer filter in perpendicular direction + spectral filter + WFPC2 + HST. If the user does not specify these, they will be estimated from look-up tables.

b) There is a switch which controls whether the mean transmission of the pick-off mirror is multiplied into the results. This prevents pick-off mirror transmission from appearing twice in the photometric correction (i.e. once if SYNPHOT is used to convert counts to flux, and again in the Mueller matrices).

c) WFPC2 spectral filter and wavelength setting, if the LRF filter is used.

d) Up to 3 sets of [polarizer / aperture, polarizer filter, PA_V3, and observed counts] may be input. The polarizer / apertures are selected by choosing from a menu.

The following steps are performed during calculation:

1) For the first (polarizer / aperture, polarizer filter, PA_V3) setting, compute the Mueller matrix for HST rotation using supplied PA_V3.

2) Get filter mean wavelength from look-up table (or just use LRF wavelength). Look up pick-off mirror reflectances and phase retardance for that wavelength. Compute attenuation matrix for pick-off mirror from physical constants.

3) Compute the angle between the pick-off mirror axis and the polarizer filter axis using (aperture / filter) chosen by user. Compute Mueller matrix for rotation.

4) Look up polarizer transmissions for mean wavelength of the spectral filter. If user has input SYNPHOT results for the polarizer, use those instead. Compute Mueller matrix for polarizer.

5) Multiply the four Mueller matrices together, thus arriving at a single 4x4 matrix for the entire system. Apply scalar correction for mean pick-off mirror transmission, if switch was set to “yes.”

6) Loop back to (1) for the second and third combinations of (polarizer aperture, polarizer filter, PA_V3) input by the user.

7) Since the CCD is only sensitive to Stokes I, and since we assume Stokes V=0, harvest the first three elements of the top row of each Mueller matrix, and pack into a 3x3 matrix. This matrix effectively gives the three count rates input by the user as a function of the Stokes I, Q, and U parameters of the wavefront, thus forming a system of three equations in three unknowns.

8) Invert 3x3 matrix using procedure based on Bevington’s MATINV to give Stokes I, Q, and U as function of the counts input by the user.

9) Extract Stokes I from current Stokes vector, which is what CCD detects. If user gave SYNPHOT results, apply the spectral filter result to I, and divide by the mean pick-off mirror transmission. Output these equations for I, Q, and U.

10) If the user has actually input counts, solve for and output I, Q, U, fractional polarization p, and E-vector position angle χ.